POWER SPECTRA OF GEOMAGNETIC FLUCTUATIONS BETWEEN 0.1 AND 10.0 HZ

John Michael Barry

NAVAL POSTGRADUATE SCHOOL
Monterey, California

THESIS

Power Spectra of Geomagnetic Fluctuations
Between 0.1 and 10.0 Hz

by

John Michael Barry

June 1978

Thesis Advisor: O. Heinz

SECURITY CLASSIFICATION OF THIS PAGE (When Data Entered)

REPORT DOCUMENTATION PAGE		READ INSTRUCTIONS BEFORE COMPLETING FORM
1. REPORT NUMBER	2. GOVT ACCESSION NO.	3. RECIPIENT'S CATALOG NUMBER
4. TITLE (and Subtitle) Power Spectra of Geomagnetic Fluctuations between 0.1 and 10.0 Hz		5. TYPE OF REPORT & PERIOD COVERED Master's Thesis: June 1978 6. PERFORMING ORG. REPORT NUMBER
7. AUTHOR(s) John Michael Barry		8. CONTRACT OR GRANT NUMBER(s)
9. PERFORMING ORGANIZATION NAME AND ADDRESS Naval Postgraduate School Monterey CA 93940		10. PROGRAM ELEMENT, PROJECT, TASK AREA & WORK UNIT NUMBERS
11. CONTROLLING OFFICE NAME AND ADDRESS Naval Postgraduate School Monterey CA 93940		12. REPORT DATE June 1978 13. NUMBER OF PAGES 69
14. MONITORING AGENCY NAME & ADDRESS(if different from Controlling Office) Naval Postgraduate School Monterey CA 93940		15. SECURITY CLASS. (of this report) Unclassified 15a. DECLASSIFICATION/DOWNGRADING SCHEDULE
16. DISTRIBUTION STATEMENT (of this Report) Approved for public release; distribution unlimited.		
17. DISTRIBUTION STATEMENT (of the abstract entered in Block 20, if different from Report)		
18. SUPPLEMENTARY NOTES		
19. KEY WORDS (Continue on reverse side if necessary and identify by block number)		

20. ABSTRACT (Continue on reverse side if necessary and identify by block number)
An optically pumped Cesium vapor magnetometer was used to measure the temporal fluctuations of the total geomagnetic field at Monterey, California. Power spectra were obtained from these recordings for the frequency range 0.1-10 Hz. Measurements were made during the month of April 1978 with the Kp index varying from 0+-8+. The power spectra obtained displayed a characteristic -20 dB/decade slope from 0.1-2.0 Hz and were essentially flat between 2.0-10 Hz. Measurement times were: Local night (0000-0200),

DD FORM 1 JAN 73 1473 EDITION OF 1 NOV 65 IS OBSOLETE
S/N 0102-014-6601 |

SECURITY CLASSIFICATION OF THIS PAGE (When Data Entered)

local morning (0800-1000) and local afternoon (1600-1800). Local morning exhibited the highest power density levels, exceeding the lowest power density levels (recorded during local night) by 10dB at .1 Hz and 3dB at 10 Hz. A comparison of a magnetically disturbed day (Fredricksburg a index of 7) with a magnetically quiet day (Fredricksburg a index of 3) showed that at the low frequency end of the spectrum (.1-.6 Hz) there was 10dB more power on the disturbed day.

Approved for public release; distribution unlimited

Power Spectra of Geomagnetic Fluctuations Between 0.1 and 10.0 Hz

by

John Michael Barry
Lieutenant, United States Navy
B.S.E.E., United States Naval Academy, 1971

Submitted in partial fulfillment of the
requirements for the degree of

MASTER OF SCIENCE IN PHYSICS

from the

NAVAL POSTGRADUATE SCHOOL

June 1978

ABSTRACT

An optically pumped Cesium vapor magnetometer was used to measure the temporal fluctuations of the total geomagnetic field at Monterey, California. Power spectra were obtained from these recordings for the frequency range 0.1 - 10 Hz. Measurements were made during the month of April 1978 with the Kp index varying from 0+ - 8+. The power spectra obtained displayed a characteristic -20 dB/decade slope from 0.1 - 2.0 Hz and were essentially flat between 2.0 - 10. Hz. Measurement times were: Local night (0000-0200), local morning (0800-1000) and local afternoon (1600-1800). Local morning exhibited the highest power density levels, exceeding the lowest power density levels (recorded during local night) by 10dB at .1 Hz and 3dB at 10 Hz. A comparison of a magnetically disturbed day (Fredricksburg a index of 7) with a magnetically quiet day (Fredricksburg a index of 3) at the same local time (1730-1930) showed that at the low frequency end of the spectrum (.1 - .6 Hz) there was 10dB more power on the disturbed day.

TABLE OF CONTENTS

LIST OF FIGURES

ACKNOWLEDGEMENT

While a number of persons contributed directly and indirectly to this report, special thanks must go to Dr. Otto Heinz, my advisor for this project, who offered his guidance whenever it was needed.

I am also greatly indebted to Dr. Paul Moose who made sense out of the Physics and who spent a good deal of time in the woods helping me search for greater signal/noise.

Finally, to Mr. Bob Smith of the Research Department for his valuable assistance in getting the equipment and making it run, I offer my sincere thanks.

I. INTRODUCTION

It is often convenient to consider the geomagnetic field as made up of two major components: (1) The main field which can be considered to be approximately dipole and generated in the interior of the earth, and whose observable temporal fluctuations are on the order of years or longer. For purposes of this study, we shall consider the main geomagnetic field to be constant in time. (2) A time-varying component superimposed on the main geomagnetic field whose origin is to be found in the ionosphere and the magnetosphere. This time-varying component of the geomagnetic field is of small amplitude compared to the main field (1 part in 10^4 or less) and involves frequency components up to the kHz range.

The study of this time-varying component of the earth's magnetic field is of interest in gaining a better understanding of basic geophysical processes as well as in improving the performance of existing or projected devices which are employed by the Navy. A number of operational Navy systems such as M(agnetic) A(nomaly) D(etection), magnetic mines, torpedoes and others, as well as some projected systems (such as ELF Communication Systems), depend on the detection of small changes in the existing magnetic field in the ocean. Thus, from both a scientific and a Naval applications point of view, detailed experimental data on the geomagnetic field fluctuations seem highly desirable.

As a first step in an experimental program to characterize and understand more fully the magnetic field fluctuations in and near the ocean, we have measured the power spectrum of the fluctuations in Monterey, California using an optically pumped, total field magnetometer. The measurements were carried out at a relatively quiet field site near La Mesa village. A total of 52 hours of geomagnetic field recordings were made, at various times of day and under varying conditions of geomagnetic activity. Frequency analysis was performed on the data yielding the power spectrum of the fluctuations in the frequency range of 0.1 to 10.0 Hz. The general shape of the power spectra agrees with earlier measurements but several novel features were also observed.

II. BACKGROUND

A. SOURCES OF GEOMAGNETIC FLUCTUATIONS

Figure 1 shows an approximate power spectrum of the fluctuations measured on the earth's surface and having periods of a day or shorter. Also indicated on the graph are the approximate amplitudes of the field fluctuations showing that even the largest of these fluctuations are less than 1 percent of the magnitude of the Main Field ($B \approx 50{,}000$nT). Nevertheless, they are of considerable interest both from the point of view of geophysics and from the point of view of Navy applications, and a world-wide network of magnetic observatories maintains continuous records of measurements of these varying field components. World Data Center A (operated by NOAA in Boulder, Colorado) issues several indices as well as forecasts of geomagnetic activity on a daily basis.

The major diurnal variations have a period of 24 hours and are caused by current systems generated in the upper atmosphere as a result of solar heating. At mid-latitudes this Sq effect tends to be 25 - 50 nT, but in the equatorial regions, the effect of the equatorial electrojet can cause a typical variation of about one hundred nT even during magnetically quiet conditions. There also exists a much smaller diurnal variation with a period of 12 hours, caused by lunar atmospheric tides. The magnitude of this variation is less than 0.1 of the daily solar variation.

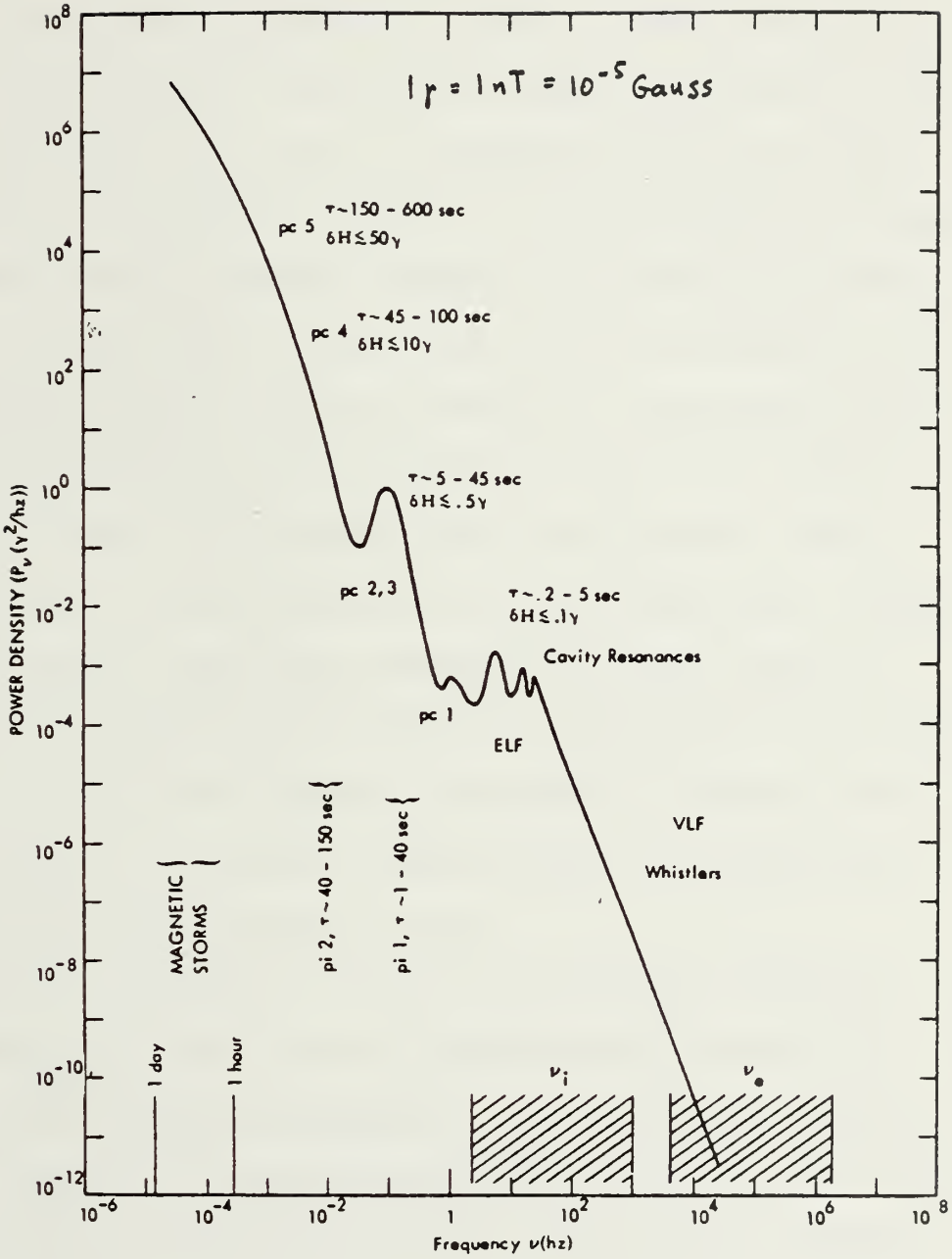

Figure 1. Power spectrum of geomagnetic disturbances observed on the Earth's surface.

[Cladis, (1977)]

Spherical harmonic analysis of these so-called Sq and L variations from a world network of observatories allows one to determine the equivalent electric current systems responsible for the observed magnetic variations. About two-thirds of the variations are found to be due to currents flowing external to the earth, and the remaining third can be attributed to currents induced in the earth's surface layers by the variable external field. The external currents are found to flow mostly at an altitude of about 100 km and are produced by convective movements of the conducting upper atmosphere across the earth's magnetic field lines. By analogy with the electric dynamo, this mechanism is often referred to as the atmospheric dynamo.

Magnetic storms, which are severe, world-wide magnetic disturbances, have their main frequency components in the same region of the spectrum as diurnal variations. However, the rate of occurrence of magnetic storms seems to be primarily influenced by the solar sunspot cycle.

Magnetograms obtained at low and mid-latitude stations indicate that many storms have a characteristic pattern of development as the storm progresses. The start of a typical storm, signalled by an abrupt world-wide increase in the horizontal component of the magnetic field, is known as a sudden commencement. This increase is typically 20 - 30 nT and has a rise time of a few minutes. The next 2 - 8 hours, during which the field remains at values higher than pre-storm, is known as the initial phase. This is followed by a 12 - 24 hour

period during which the field decreases to values typically 100 nT below its undisturbed magnitude, and this is known as the main phase. The final stage of the storm is characterized by a gradual return of the field to its pre-storm value and lasts one to three days.

Individual storm records will, of course, show deviations from this "typical storm", particularly at higher latitudes, where rapid, large-scale fluctuations are common during storms. Even at mid-latitudes large amplitude fluctuations with periods of about one-half hour are occasionally observed during the main phase of a storm.

Sudden changes in the dynamic pressure of the solar wind impinging on the outer boundary of the geomagnetic field are believed to be responsible for the initiation of magnetic storms and the subsequent development represents the response of the magnetosphere and the charged particles within it to this initial impulse.

The frequency region of greatest interest to us lies below 3 Hz, commonly known as ULF. Geomagnetic field fluctuations in this frequency region are usually referred to as micropulsations, with periods varying from 0.2 - 600 seconds, and amplitudes from a fraction of an nT at the high frequencies to several tens of nT at the low frequency end of the interval. Micropulsations are divided into two general types: Continuous or pc and irregular or pi. The pc micropulsations display amplitude variations which are quasi-sinusoidal and last

several hours, whereas pi micropulsations have considerable irregularities both in frequency and amplitude. As indicated in Figure 1, the spectrum of micropulsations has been subdivided into roughly 5 segments ranging from pc 1 at the high frequency end to pc 5 at the lowest frequencies. The occurrence of pc's has a diurnal variation with a maximum near local noon. It is believed that pc's represent small hydromagnetic disturbances existing in the daytime magnetosphere, but the possibility that they are of ionospheric origin cannot be ruled out at this time. The pi's are trains of micropulsations consisting of series of damped oscillations lasting from a few minutes to about one hour and having periods of roughly 40 - 100 seconds. Their amplitude is largest in the auroral zone and decreases with decreasing latitude, and they appear to be preferentially generated in the night-time magnetosphere. At high latitudes, there is evidence that pi's are hydromagnetic waves which have been greatly amplified by plasma instabilities created in the magnetosphere by high-energy electrons.

In the ELF frequency range (3 - 3000 Hz), a number of emissions contribute to the magnetic fields, the most pronounced ones being the earth-ionosphere cavity resonances (Schumann resonances). These signals result from disturbances that are resonantly excited by lightning transients in the concentric spherical cavity formed by the earth's surface and the lower region of the ionosphere. The power spectra of the ELF signals often show maxima near 7.8, 14.1, 20.3, 26.4 and 32.5 Hz [Schumann and König, 1954].

B. REVIEW OF EARLIER WORK

Power spectrum analysis of the geomagnetic field has been a popular tool to better understand geomagnetic field activity and to gain insight into possible source mechanisms for the fluctuations. For many naval applications one must also understand these geomagnetic phenomena, so that in attempting to detect man-made magnetic anomalies, one might try to eliminate this background signal. This allows for concentration on a smaller frequency range, which is of importance to the military observer. The next few pages are devoted to a short review of work done in power spectrum analysis of the geomagnetic field.

In 1963, Santirocco and Parker reported [Santirocco and Parker 1961] their work on the polarization and power spectra of pc[1] micropulsations. Recordings of the N-S, E-W, and vertical components of the geomagnetic field in the frequency band .005 - 5 Hz were made at a shore location in Bermuda. The field sensors utilized were ferromagnetic-cored loop antennas, polarized so that dB/dt vectors pointing North, East and down were

---

[1]Geomagnetic micropulsations are field variations with periods ranging from .2 seconds to approximately 10 minutes. A terminology recommended by the International Association of Geomagnetism and Aeronomy is pc for pulsations continuous and pi for pulsations irregular. The period ranges are:

pc 1	.2 - 5 sec	pi 1	1 - 40 sec
pc 2	5 - 10 sec	pi 2	40 -150 sec
pc 3	10 - 45 sec		
pc 4	45 -150 sec		
pc 5	150 -600 sec		

For further details see Jacobs [1970], p. 16-20.

defined as positive. The sensitivity of the loops was 70[μv-sec/nT] (where 1 nT = 1 Gamma or 10^{-5} Gauss). With 350 hours of continuous taping of the field components reported, power spectrum analysis of the tapes was carried out. The power spectra of the pc pulsations appeared as clumps of variable fine structure components superimposed on a residual background which falls monotonically with a slope of -6dB/ octave. Santirocco and Parker also observed that upon comparison with the results of others that this background slope is constant from .0002 Hz to nearly 1 Hz.

Davidson reported in 1964 results on the average diurnal characteristics of geomagnetic power spectra in the period range 4.5 - 1000 seconds [Davidson 1964]. This study aimed at investigating the source and propagation mechanisms by means of the variability of the power spectral density as a function of 1) the spectral distribution of the source or driving function; 2) the coupling or impedance matching to the medium for various propagating modes, and 3) the propagation characteristics of the medium including the geometrical effects of the boundaries.

The data was taken in the New Jersey coastal plain area (geomagnetic coordinates 39° 38.5'N , 74° 31.8'W and magnetic inclination 71°), using a Rubidium vapor magnetometer. Spectra were then obtained by digital processing, using the techniques of Blackman and Tukey [1968]. From these measurements, it was found that there are empirical expressions for the power density

G(f) (in units on $[\frac{(nT)^2}{Hz}]$ as a function of period as follows:

for the 2.5 - 10.0 sec. period range the expression is

$G(f) = 1.26 \times 10^{-4} T^{1.3}$ (T in seconds).

For the greater than 10.0 sec. period range the expression is

$G(f) = 6.31 \times 10^{.6} T^{2.6}$ (T in seconds).

It was also found that these two spectral components appeared to be independent of time. In addition, these period ranges contain spectral peaks superimposed on the constant slopes at 5 sec. and 10 sec. periods. A second group of spectral peaks fall within the 17 - 70 sec. period range.

Later another study made in the same area [Herron 1967] reported that in the 1700 - 2300 hour local time frame, the power spectra had the highest overall power density levels, and the strongest spectral peaks. It was also observed that the log log plot of Power vs. Period had a slope of -7.1 dB per octave.

Recently the efforts of A.C. Fraser-Smith and J.L. Buxton [1975], using a SQUID (Superconducting Quantum Interference Device) magnetometer, enabled them to achieve higher sensitivity measurements of the geomagnetic activity in the frequency range .1 - 14 Hz. The measurements were taken at a mid-latitude location, in Stanford, California (geomagnetic latitude 43.5°N) on the N-S field component and spanned a 2-month interval between 26 January and 26 March 1974. They found a minimum in the

spectrum in the 3 - 7 Hz frequency range while in the .1 - 3 Hz range, there is a monotonic decrease with frequency. The variation is approximately $f^{-1.25}$ for the .2 - 5 Hz (pc 1) range. For the frequency range 7 - 14 Hz, the magnetic activity is dominated by the first Schumann resonance.

Finally, a report was made on the power spectrum observations made from data collected in nine induction magnetometer observatories in widely separated locations about the earth [Wertz and Campbell 1976]. It was found that the slope of the log (Power Spectral Density) vs. log (Period) was about 3 at low latitudes and 4 in the Auroral Zone. There is a maximum of power spectral density at auroral latitudes and a minimum at the lower middle latitudes. For 10 second period measurements, the power spectral density varied from 2×10^{-5} to 2×10^{-2} $(nT)^2/Hz$. For the 100 second period data, the power spectral density varied from 4×10^{-1} to 2×10^{2} $(nT)^2/Hz$. The correlation between spectral density amplitudes and sunspot number was .9 for 12 second period data taken in College, Alaska. Earth surface conductivity, ionospheric variations and magnetospheric conditions were found to control the amplitude of the signals.

In addition to these published results, there is considerable on-going work associated with various Navy projects, which involves some measurements of geomagnetic fluctuations in the frequency range considered in this report. For further details see Ref. 11, 13 and 14.

III. EXPERIMENTAL SETUP

A. GENERAL LAYOUT OF EXPERIMENT

As mentioned earlier, there are essentially two components to the geomagnetic field. These are the main field and the time-varying components superimposed on the main field. This experiment dealt with the measurement of the time-varying field exclusively, treating the main field as the stable or d.c. component.

The experiment was conducted in Monterey, California, in the community called La Mesa Village (Geomagnetic Latitude 42.5°N). The sensors for magnetic field measurement were located in an adjacent wooded area subject to relatively few magnetic field disturbances.

The measurement of the field was conducted using a Cs Vapor, optically pumped magnetometer with a pair of sensors positioned a distance of 55 meters (180 ft) apart on an East-West line. The main electronics and power supply equipment were housed in Building 318, 61 meters (200 ft) from either sensor. Electrical power to and signal from the sensors were transmitted via a coaxial cable 61 meters long.

The geomagnetic field's time variations were measured at various times both local day and night, to get a sampling of the field as a function of time of day. The general level of geomagnetic activity ranged from very quiet to disturbed during the

month of observations. Magnetic activity index Kp range was 0+ to 8+.

B. DESCRIPTION OF MAGNETOMETER

The sensing unit of the magnetometer is the Cesium Vapor cell. The operation of this sensing unit is based on the optical pumping and monitoring technique [Dehmelt 1957]. This technique has its basis in the Zeeman splitting of energy levels of the cesium valence electron in the presence of a magnetic field. The energy levels are split into sublevels which have energy differences proportional to the total intensity of the ambient magnetic field.

To measure the energy differences between the sublevels we note that $\Delta E = h\nu$ and hence a measurement of ν, the frequency of the emitted or absorbed photons determines ΔE which in turn is proportional to the ambient magnetic field B since

$$\Delta E = \frac{geh}{4\pi m} B.$$

(g = Lande g factor, e = charge on the electron, h = Planck's constant, m = mass of the electron, B = the ambient magnetic field.)

The measurement of ν is accomplished by monitoring the optical transparency of the pumped Cs vapor cell while applying a RF field slowly swept in frequency around ν. When the driving frequency corresponds to ΔE, the optically pumped electrons are redistributed among all of the sublevels leading to an increased absorption of the optical radiation. Thus at this particular

value of ν, usually called the Larmor frequency ν_L, we have

$$\Delta E = h\nu_L = \frac{geh}{4\pi m} B \text{ or } \nu_L = \frac{ge}{4\pi m} B$$

The constant of proportionality between the Larmor frequency and the magnetic field intensity for cesium is 3.499 Hz/nT. The cesium sensor actually detects the magnetic field strength by monitoring the transmission of resonance radiation through the optically pumped cesium vapor cell, and produces a signal whose frequency is proportional to the total magnetic field intensity (with very fast response even to large field changes). Figure 2 illustrates the major components of the cesium sensor. A more detailed description of the optically pumped magnetometer is given in Bloom [1961].

The cesium sensor employed throughout this experiment was of the single cell design, which has large dead zones. This means that the sensor can only detect the magnetic field when the sensor axis is within the prescribed cone in relation to the total field vector to be measured. Figure 3 illustrates the active zones of the single cell sensor and shows that they include the greater part of one hemisphere. Optimum signal to noise ratio is achieved when the optical axis of the sensor is 45° from the total field vector. Figure 4 shows the proper alignment of a signal cell sensor in the geomagnetic field, for maximum signal to noise considerations.

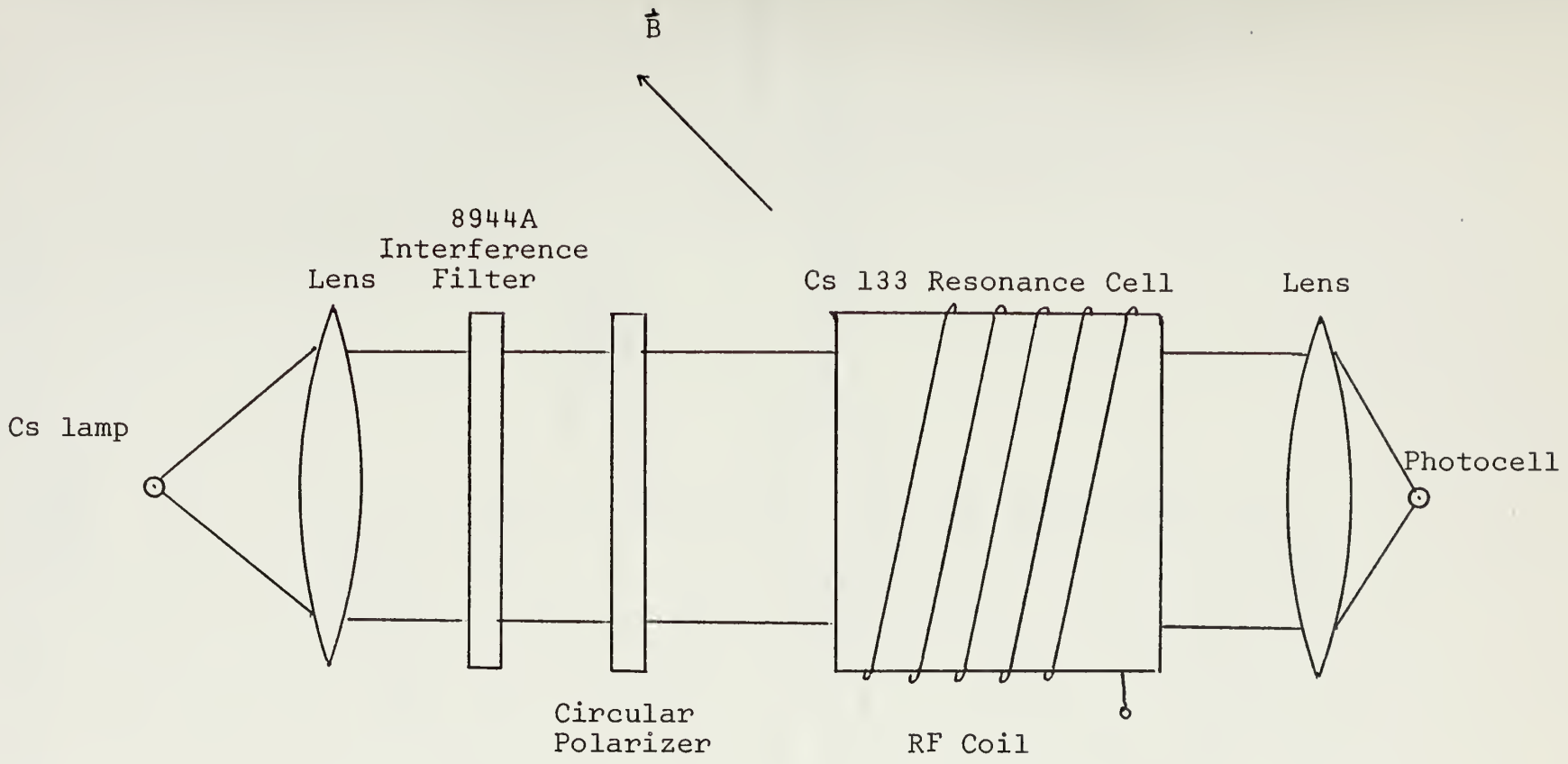

Figure 2

Major Components of Cesium Sensor

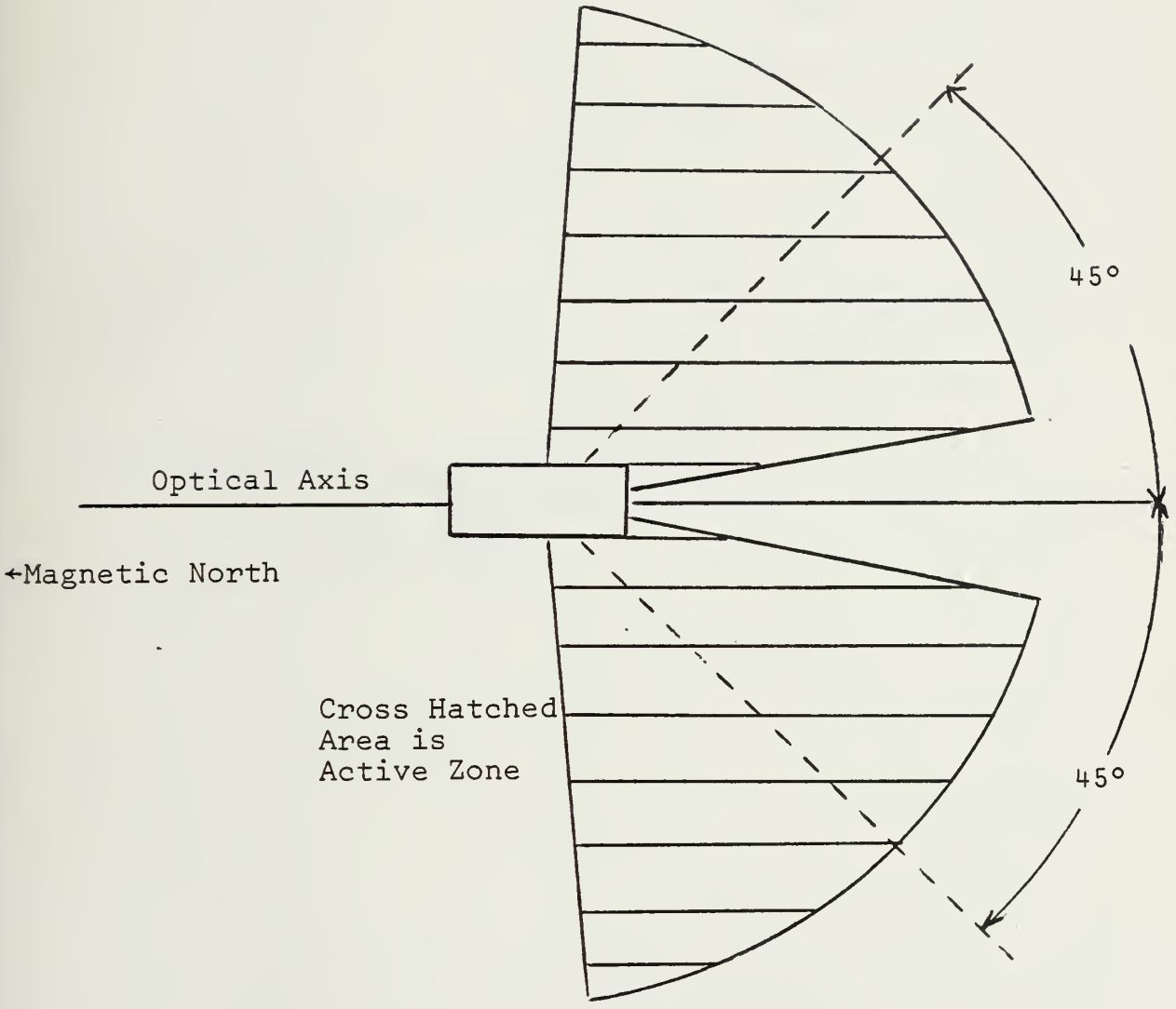

Figure 3

Active Zones of Single Cell Sensor

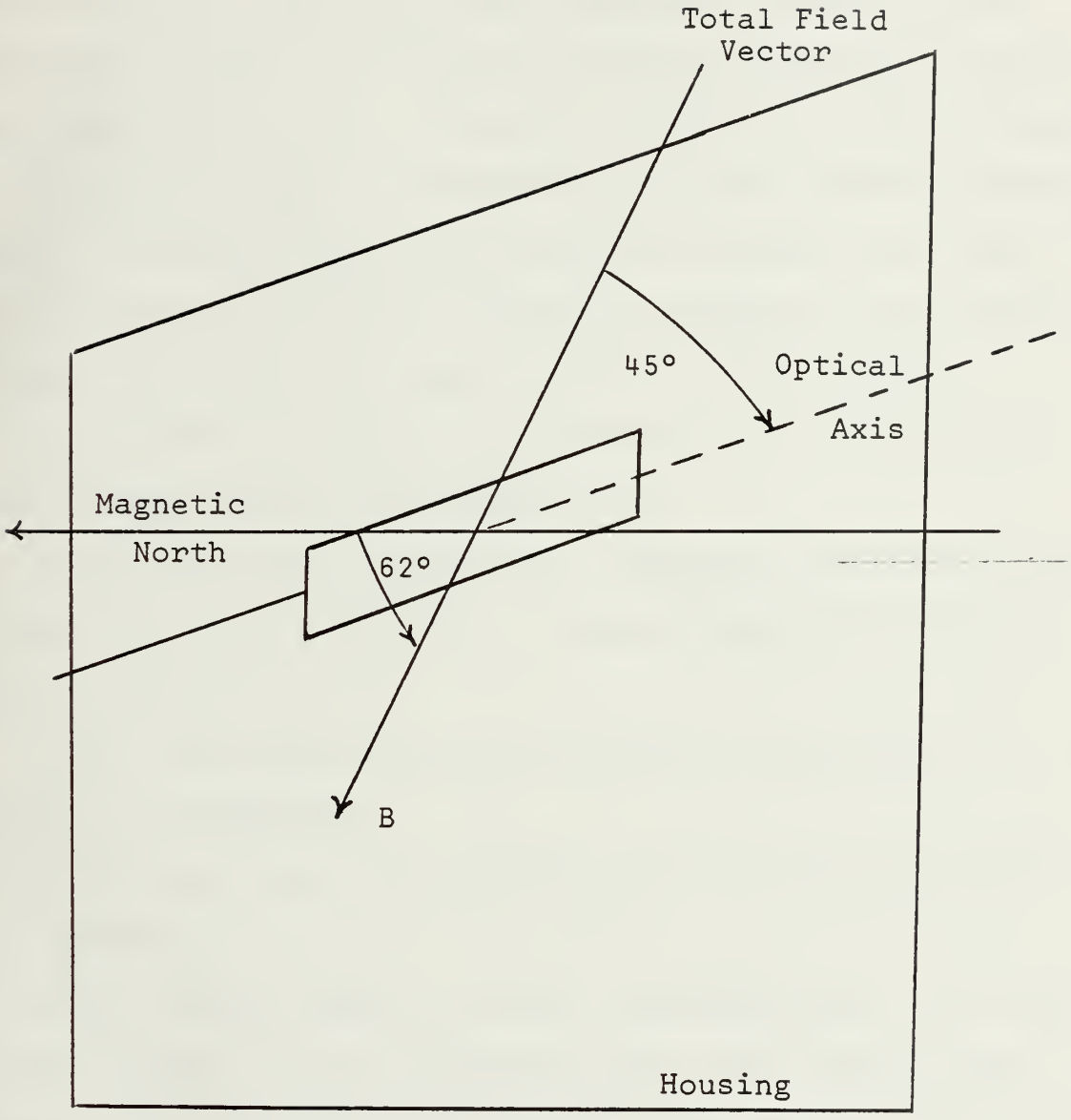

Figure 4

Sensor - Magnetic Field Geometry

The sensor is effectively an oscillator which produces an rf signal (Larmor Frequency) directly proportional to the total field intensity. Thus the Larmor Frequency provides direct information on the field and can be used in conjunction with a simple frequency counter. However, the more customary arrangement is shown in Figure 5, indicating that the Larmor Frequency signal is converted to a slowly varying voltage, whose amplitude is proportional to the frequency excursion of the Larmor Frequency, and hence the magnetic field at the sensor.

Finally, the following procedures had to be followed for reliable magnetometer system operation:

(1) The sensor was mounted in a relatively noise-free area, secluded from power lines, etc., and positioned on a firm non-magnetic support;

(2) The sensor was securely fastened to the support to preclude its movement;

(3) The cable end of the sensor was pointed in the magnetic North direction;

(4) For optimum signal to noise considerations, the sensor axis was aligned at a 45° angle from the total field vector (Magnetic Latitude 42.5°N and magnetic inclination = 62° for Monterey, California);

(5) The sensor was extended the full six feet from the sensor electronics box, and

(6) The sensor and sensor electronics units were sealed in fiberglass housings to prevent water intrusion and provide shelter from the wind.

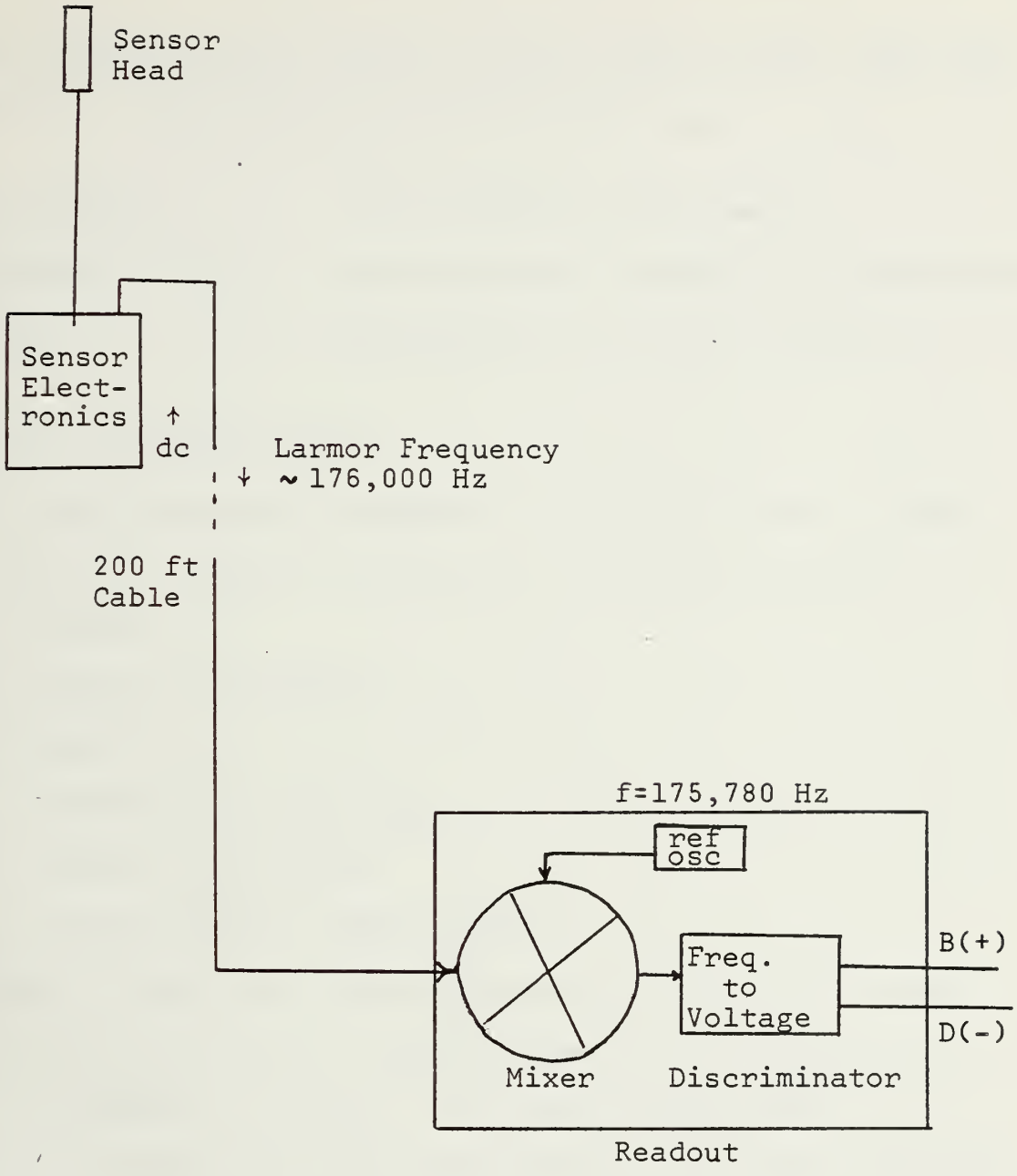

Figure 5

Magnetometer System

The specifications supplied for the Varian Model 4938 magnetometer by Varian Associates are listed here:

Sensitivity	±5 picotesla (.005 gamma)
Information Rate	Continuous and essentially instantaneous
Range	Continuous from 20,000-80,000 nT

C. DATA COLLECTION SYSTEM

The major components required to record the data on magnetic tape for analysis and display at a later time are:

(1) Sensor;

(2) Sensor Electronics;

(3) Readout;

(4) Differential Amplifier;

(5) Output Filter, and

(6) Instrumentation Tape Recorder.

Figure 6 shows the system components required to collect magnetic field data as an analog signal (i.e., voltage amplitude as a function of field). In this configuration, it is possible to tape record the analog signal for further analysis. Real time processing can be carried on simultaneously with tape recording. A comparison of the two spectra allows determination of the tape recorder noise.

In this data acquisition configuration called the magnetometer mode, the sensor generates the Larmor Frequency which is proportional to the ambient magnetic field. In the Readout, the Larmor Frequency is mixed with a reference oscillator in

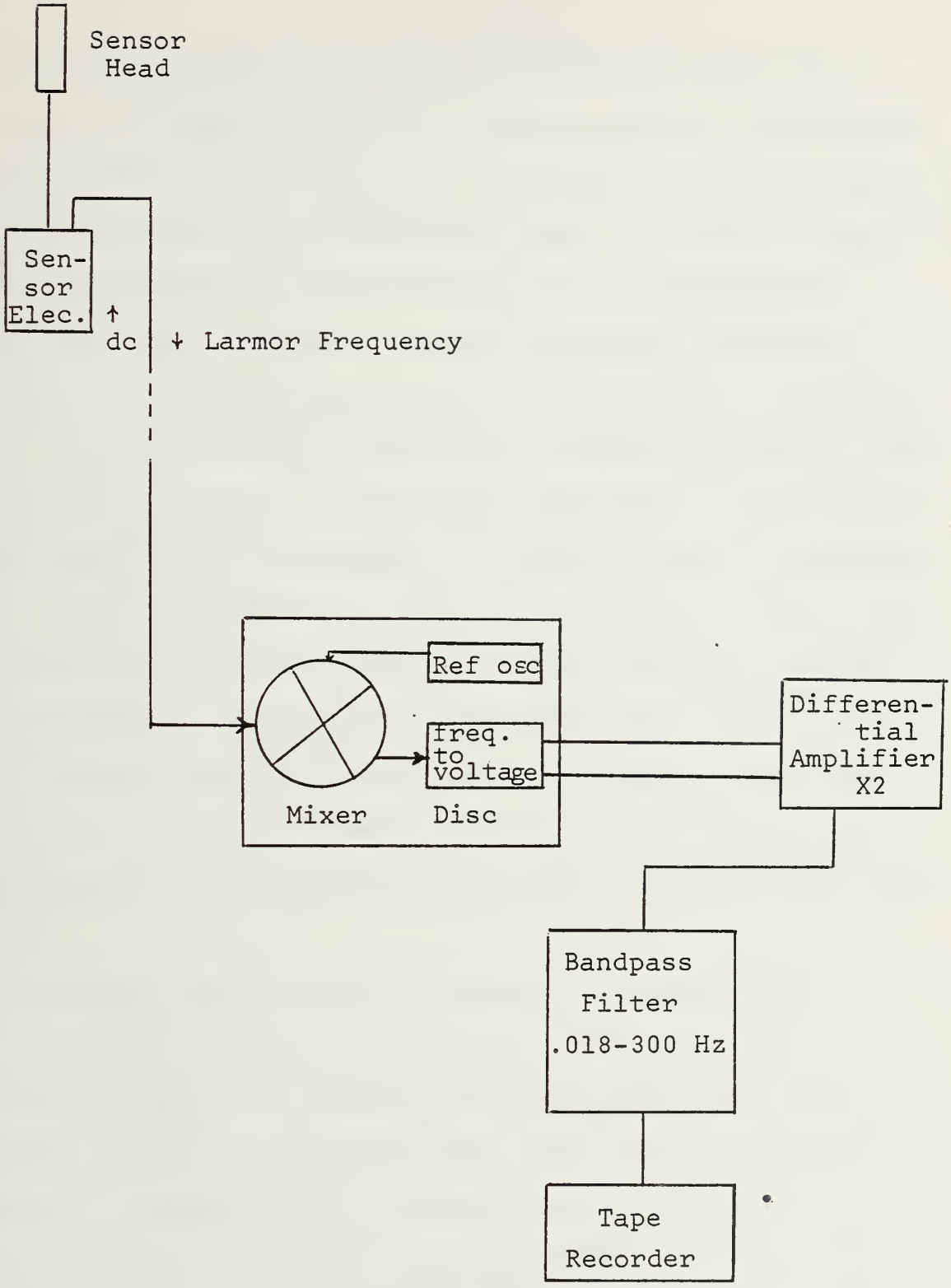

Figure 6

Data Collection System

the mixer. The frequency of the reference oscillator corresponds to the main field at the given location. In Monterey a reference oscillator frequency of 175,780 Hz corresponding to a 50.3 μT setting on the Readout was used. The mixer signal is a square wave having a frequency equal to the difference between the Larmor Frequency and the reference oscillator frequency. This square wave is the input to the discriminator driver and discriminator, and thus the change in magnetic field is converted to a d.c. voltage whose amplitude is proportional to the magnetic field variation. In order to use the discriminator output, a differential amplifier is used to accept the discriminator's balanced output (balanced output has neither side grounded). The output of the differential amplifier is then filtered (Bandlimited to .018-300 Hz) providing a suitable signal for analog magnetic tape recording. Thus this system measures the variation in the total magnetic field intensity.

The signal was recorded on a Hewlett Packard 3960 instrumentation tape recorder at a speed of 3 3/4 i.p.s. The flutter compensation option was employed to reduce the noise due to vibrations in and near the recorder. The signal sent to the recorder was a bandlimited (.018-300 Hz) analog output from the discriminator via the differential amplifier and the filter. The bandpass filter had slopes on low and high ends of 24dB/octave. All data was recorded on Scotch Brand instrumentation tape, with each side holding 2 hours and 2 minutes of magnetic

field fluctuation data. All tapes were degaussed prior to using them in data collection. The data was recorded in the FM recording mode, which improves amplitude accuracy, and is less sensitive to tape imperfections.

Some of the pertinent specifications for the tape recorder are listed below:

Carrier center frequency at 3 3/4 i.p.s.	6.75 kHz
Pass band	0 - 1250 Hz
S/N ratio without flutter compensation	48
Distortion	Less than 1.5%
d.c. drift	$\pm$.1% peak to peak output/degree Celsius

D. SCHLUMBERGER MODEL 1510-03 SPECTRUM ANALYZER

This spectrum analyzer is a fully-digitalized high performance instrument that provides real time spectrum component analysis of analog or digital input signals in 256 spectral bins across one of 10 selectable frequency bands. The result of each of the 256 independent analyses performed by the instrument is displayed on an internal C.R.O. as a dot indicating the power and frequency components of the analysis. The bandwidth of each line of resolution is dependent on the maximum frequency of the selected analysis range. The 1510 translates time domain signals into the frequency domain by Fourier transform techniques.

There are five selectable input range attenuation switches varying from .1 V_{rms} to 10 V_{rms} full scale. In addition, the 1510 has power spectrum averaging selection controls to average as many as 1024 individual spectra.

The analyzer has an option of two window functions for application to the data in the time domain, as an amplitude function multiplied by the data samples. In effect, the entire analysis sequence is amplitude modulated by the window function and the result transferred to the Digital Fourier Transform analysis memory. The window function is unity for the rectangular, and for the Hamming function $\frac{1}{2}-\frac{1}{2}\cos 2\pi \frac{n-\frac{1}{2}}{1024}$ for each n of the 1 to 1024 data samples. The rectangular window has a smaller equivalent noise bandwidth and was thus employed in the data analyzing scheme.

For the data analyzed in this experiment, the 1510 spectrum analyzer was used in one configuration only with the following settings kept constant for each sample:

Input Attenuation	.1 V_{rms} (0dB)
Frequency Range	.1 - 25.6 Hz
Window Function	Rectangular
Mode	Continuous
Spectrum Axis	X- $\log_{10} f$; Y-dB
Stop after N	depressed
Averaging Interval	512

E. CALIBRATION AND SYSTEM TESTS

A number of system tests were performed prior to data collection. The first of these tests involved the frequency response of the magnetometer system. This test was designed to check the output of the discriminator of the readout by applying a known input to the sensor head. To accomplish this task the sensor and readout were set up as illustrated in Figure 6. Measured field changes were produced and applied to the sensor by a sinusoidally stimulated 72 turn coil. A sinusoidally varying magnetic field component was generated by an a.c. current of known amplitude and frequency flowing through the coil located as shown in Figure 7.

The measured resistance of the coil was 1.1 ohms. The inductance of the coil was calculated from the equation for inductance for a circular cross section coil.

$$L_o = N^2 r \mu_o [\ln(\frac{8r}{a}) - 2] \text{ henries}$$

where N = number of turns = 72

r = radius of coil = 33×10^{-2} m

a = radius of circular cross section = 1×10^{-2} m

μ_o = permeability of free space = $4\pi \times 10^{-7} \frac{m\text{-}Kg}{s^2 A^2}$

The inductance was calculated to be 7.7 mhenries. This set up a simple circuit for the stimulation process as shown in Figure 8. The impedance ($X = R+\omega L$) is a function of frequency (ω) and the magnetic field generated by the coil is directly proportional to the magnitude of the current in the coil for

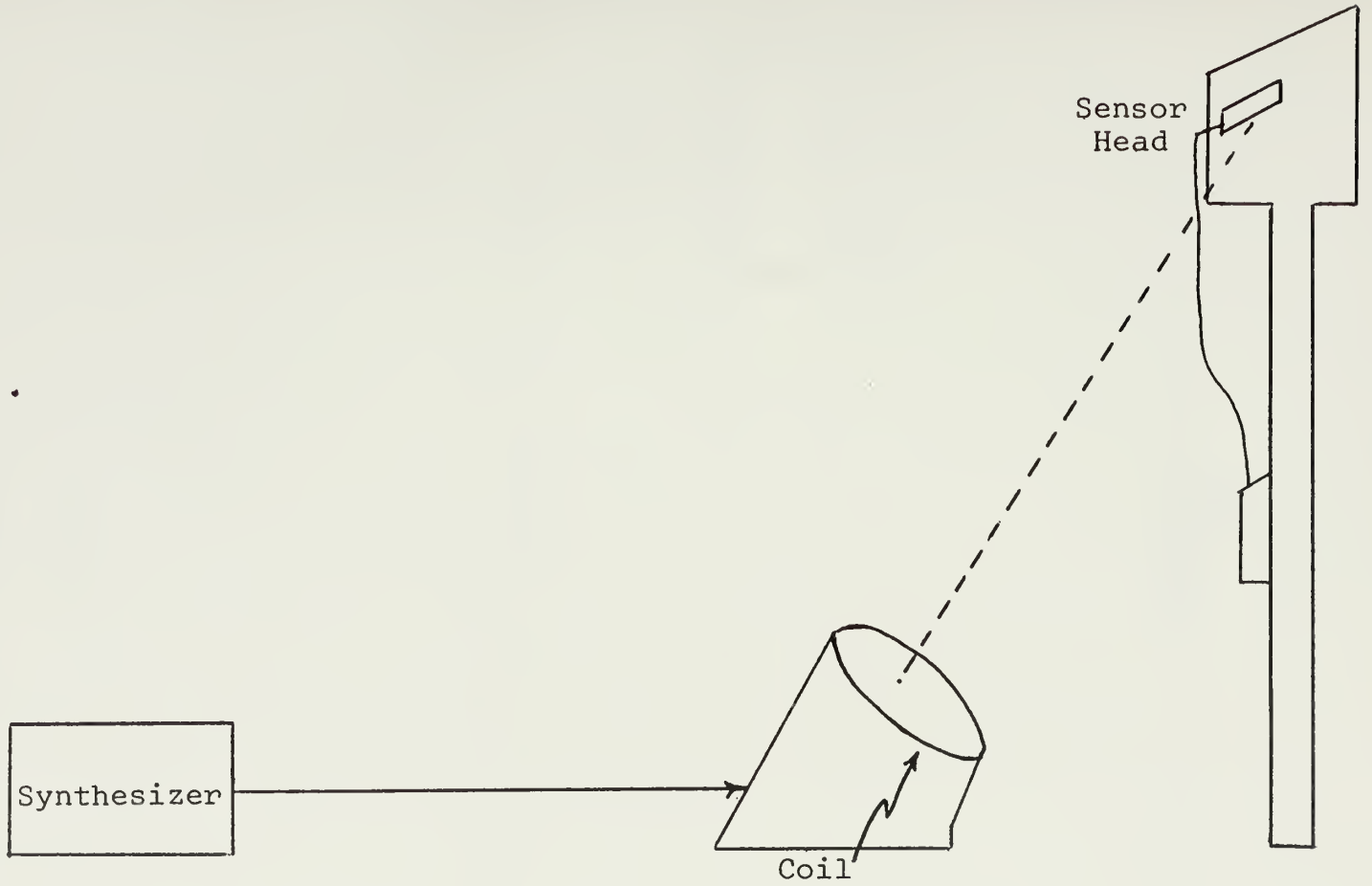

Figure 7

Coil and Sensor Geometry used to Disturb the Field

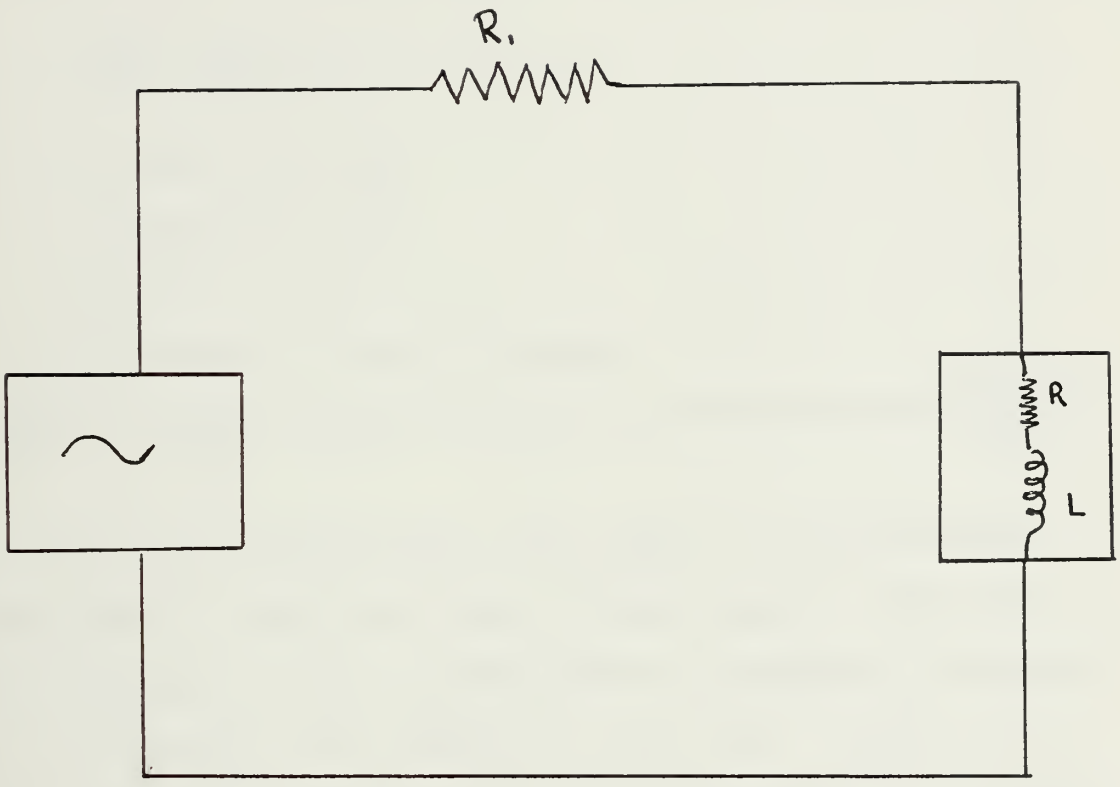

Figure 8

Circuit Diagram for
Magnetic Field Generation

the geometry described in Figure 7. Here the generated field lies along the earth's total field vector so that the coil's field either adds or subtracts from the total field vector. The magnetic field intensity along the coil axis is given by:

$$H = \frac{NIr^2}{2l^3} \frac{4\pi}{10^{-2}} \text{ [nT]}$$

where N = number of turns

I = current in coil

r = radius of coil

l = distance of coil to sensor

$\frac{4\pi}{10^{-2}}$ = factor required for unit conversion from $\frac{\text{amp-turn}}{\text{meter}}$ to nT

The coil was "swung" with a sine wave of known frequency and amplitude to change the field a known amount. The field magnitude change was kept constant while varying the frequency. Figure 9 illustrates the results of this test. Clearly there appears to be a non-linearity of system response with frequency. The test was performed on two sensors with essentially identical results. It was noted that the frequency response was essentially flat from .1 to 2 Hz, for both sensors tested. The observed roll off from 2. to 10. Hz was approximately 1.1 dB per Hertz. The exact reason for this non-linearity is not known, but an appropriate correction for it was applied to the data.

The next test involved determination of the noise level of the tape recorder that was used in data collection. This was

Figure 9

Frequency Response Curve

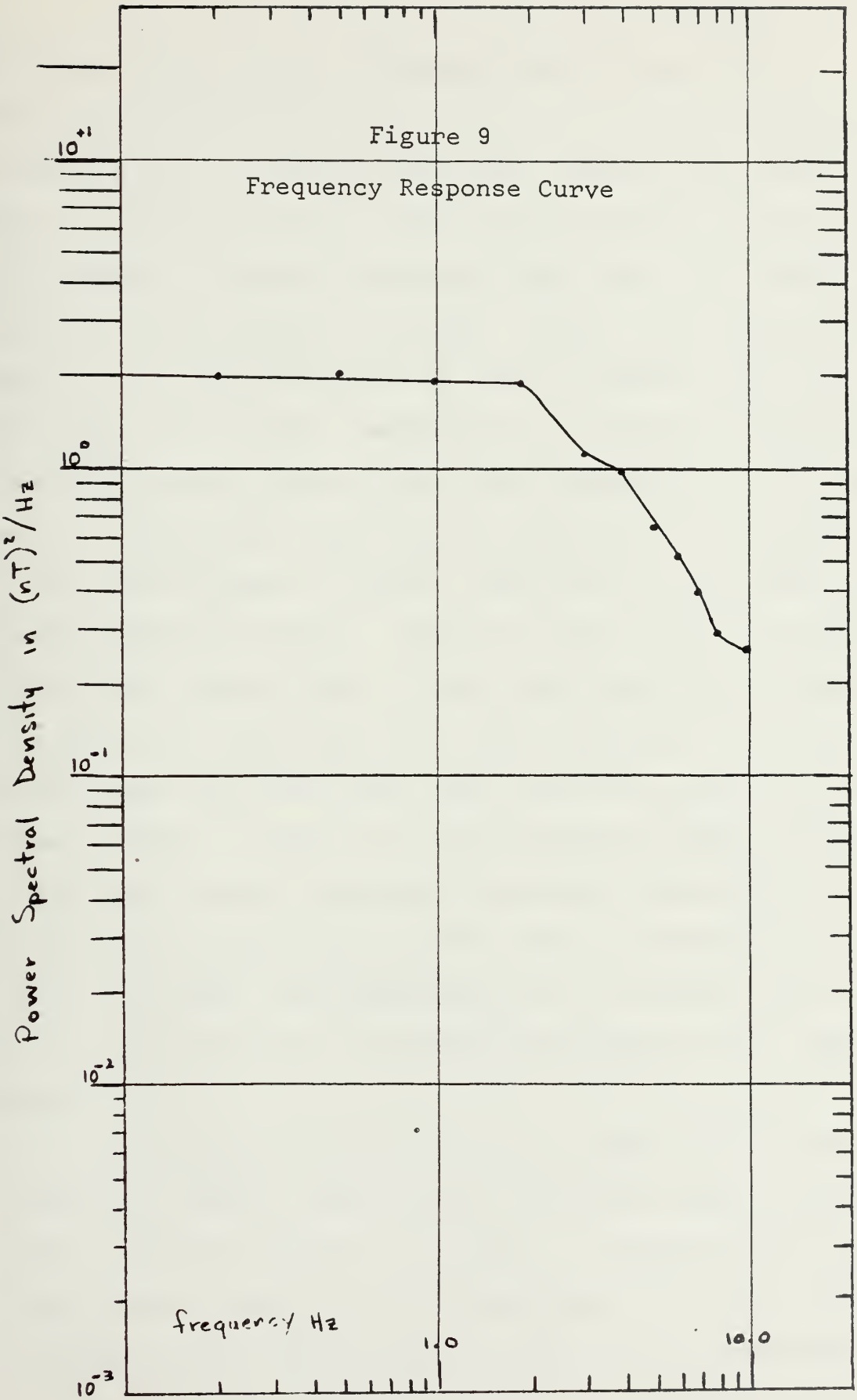

done in two ways. First a grounded input was applied to channel No. 1 of the tape recorder and the frequency spectrum was analyzed by the spectrum analyzer. Results are found in Figure 10. The analysis was run at tape recorder speed 3 3/4 i.p.s. through a bandpass filter set for range .1 to 250 Hz. The spectra were averaged 256 times. Major noise components appeared at frequencies above the area of interest and were mostly power line (60 Hz) components or power line harmonics.

Another test was used to check the reliability of the tape recorder to reproduce a given analog magnetic field signal. This test was designed to observe distortion of the signal by the tape recording process. Figure 11 gives the system components in block diagram form. A real time spectrum analysis was run while the same signal was tape recorded. The tape recorded signal was then played back and also analyzed by the spectrum analyzer. Graphs of the two spectra appear on Figure 12. The tape recorded spectrum essentially duplicated the real time spectrum and the tape recorded curve is within ± 2 dB of the direct spectrum. The small spike at 3.3 Hz was later eliminated by using the flutter compensation feature of the tape recorder.

It is not possible to put the cesium sensor into a field free region to measure sensor noise, since the sensor requires at least a 20,000 nT field to function. A readout noise measurement was possible however. This measurement was made prior to data taking, during data taking and again at its completion.

Figure 10

Grounded Input Tape Recorder Noise

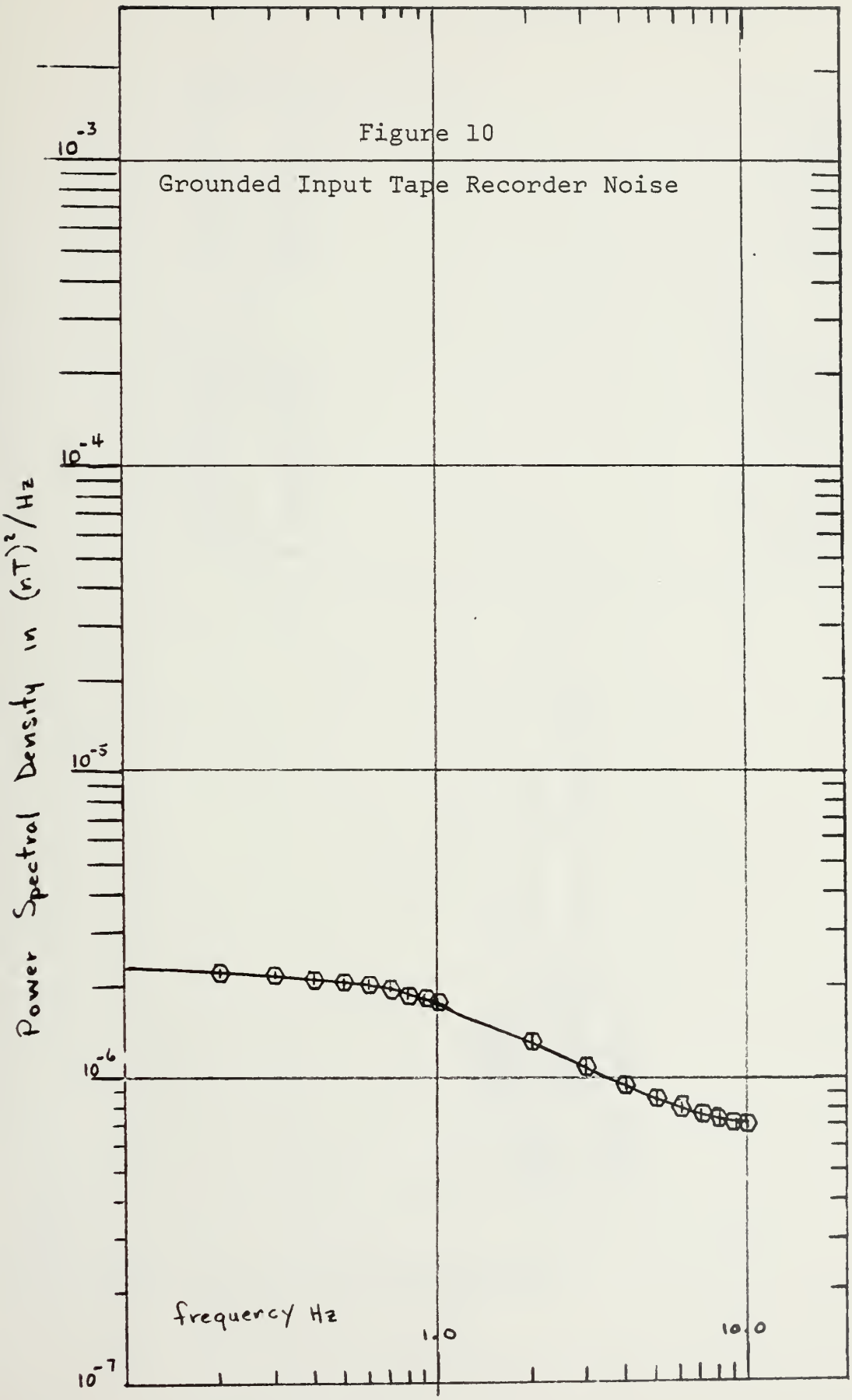

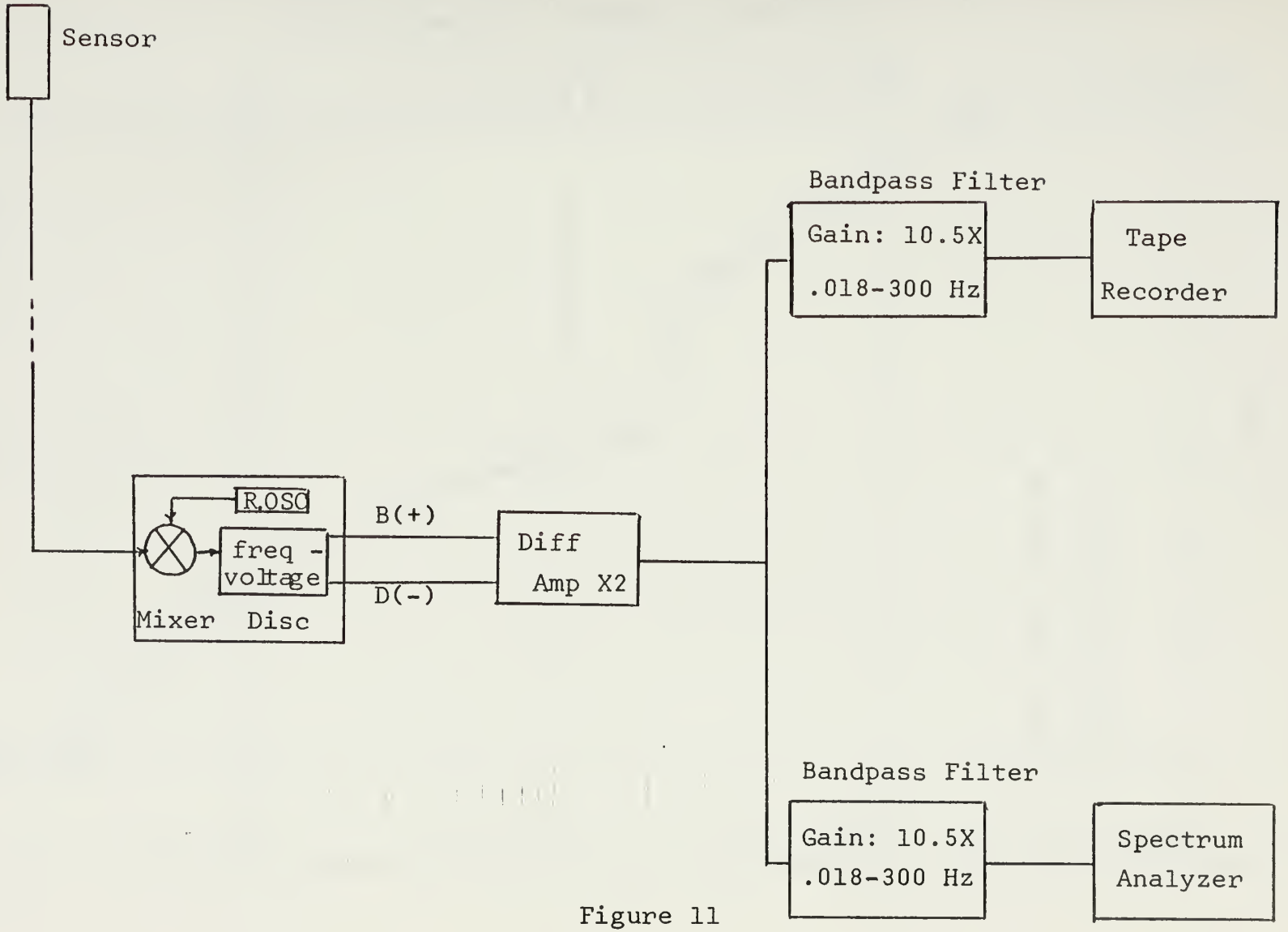

Figure 11

Tape Recorder Noise Test System

Figure 12

Tape Recorded vs. Real Time Signal

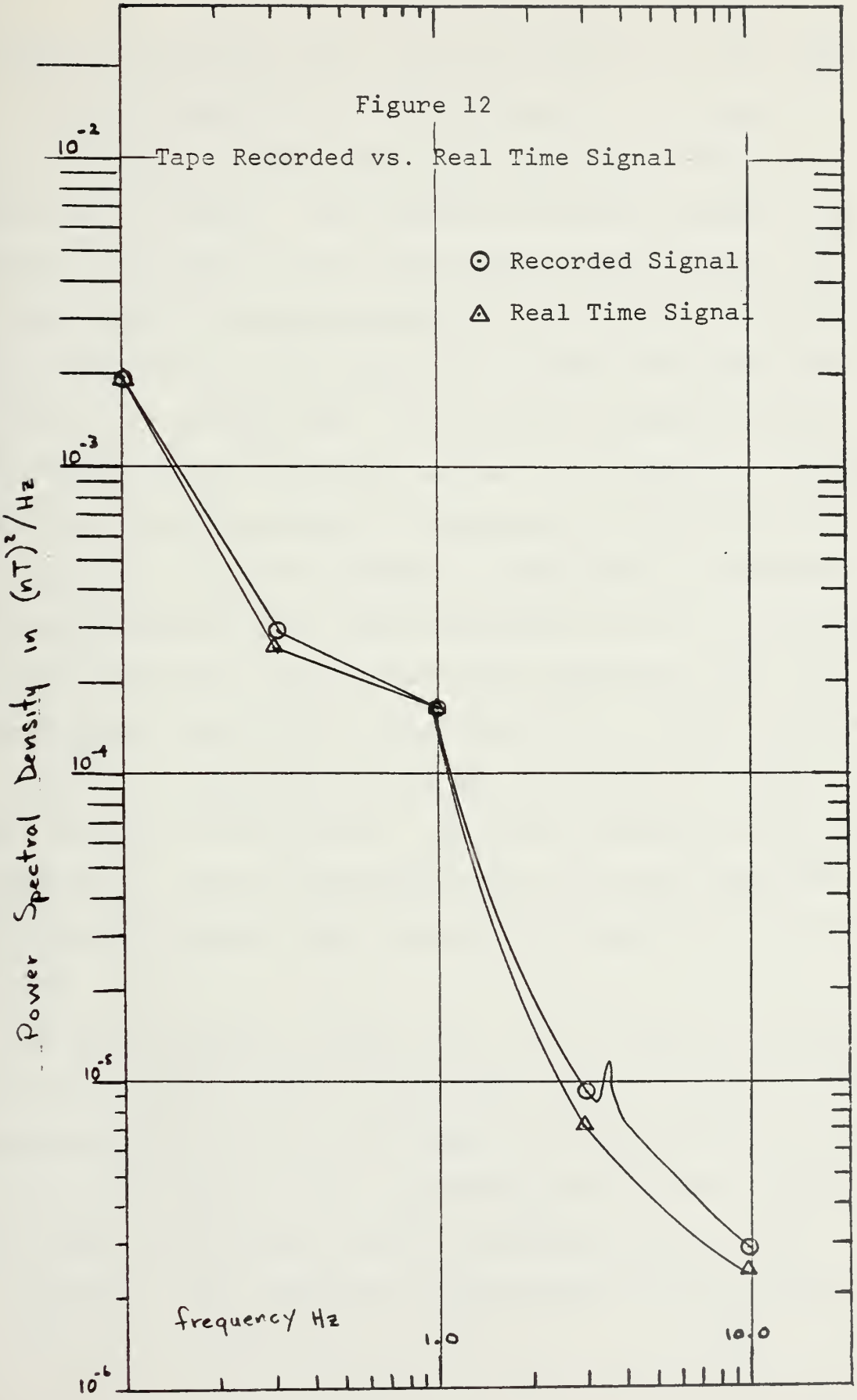

In order to obtain equipment noise associated with the readout, filter and amplifiers, it is necessary to provide a constant frequency signal input as a replacement for the varying sensor signal. This constant frequency signal must be within the range of the total magnetic field present, so that the correct reference oscillator is selected. With the sensor disconnected, the synthesized "Larmor Frequency" was applied to the readout unit. The constant frequency synthesized "Larmor Signal" was beat against the reference oscillator in the mixer and the change in frequency is detected by the discriminator. Since the change in frequency is essentially zero, there should be no signal emanating from the discriminator. This test will display any noise generated within the discriminator, mixer, filter and amplifiers. Figure 13 shows the results of an averaged noise spectrum taken over six periods within the span of one month. The noise spectrum is thus quite reproducible. The low frequency end of the noise spectrum exhibited the highest power content and dropped off by 20 dB at 10 Hz.

The power spectra obtained from the 1510 spectrum analyzer give only a relative dB scale on the y axis. It was necessary to calibrate the y axis to the power spectral density in γ^2/Hz or $(nT)^2/Hz$. This was done following the procedure outlined in the EMR 1510 Spectrum Analyzer Operators Manual. The $\log_{10}\frac{(nT)^2}{Hz}$ vs. $\log_{10}$(frequency) calibration is given here:

Figure 13

System Noise Spectrum

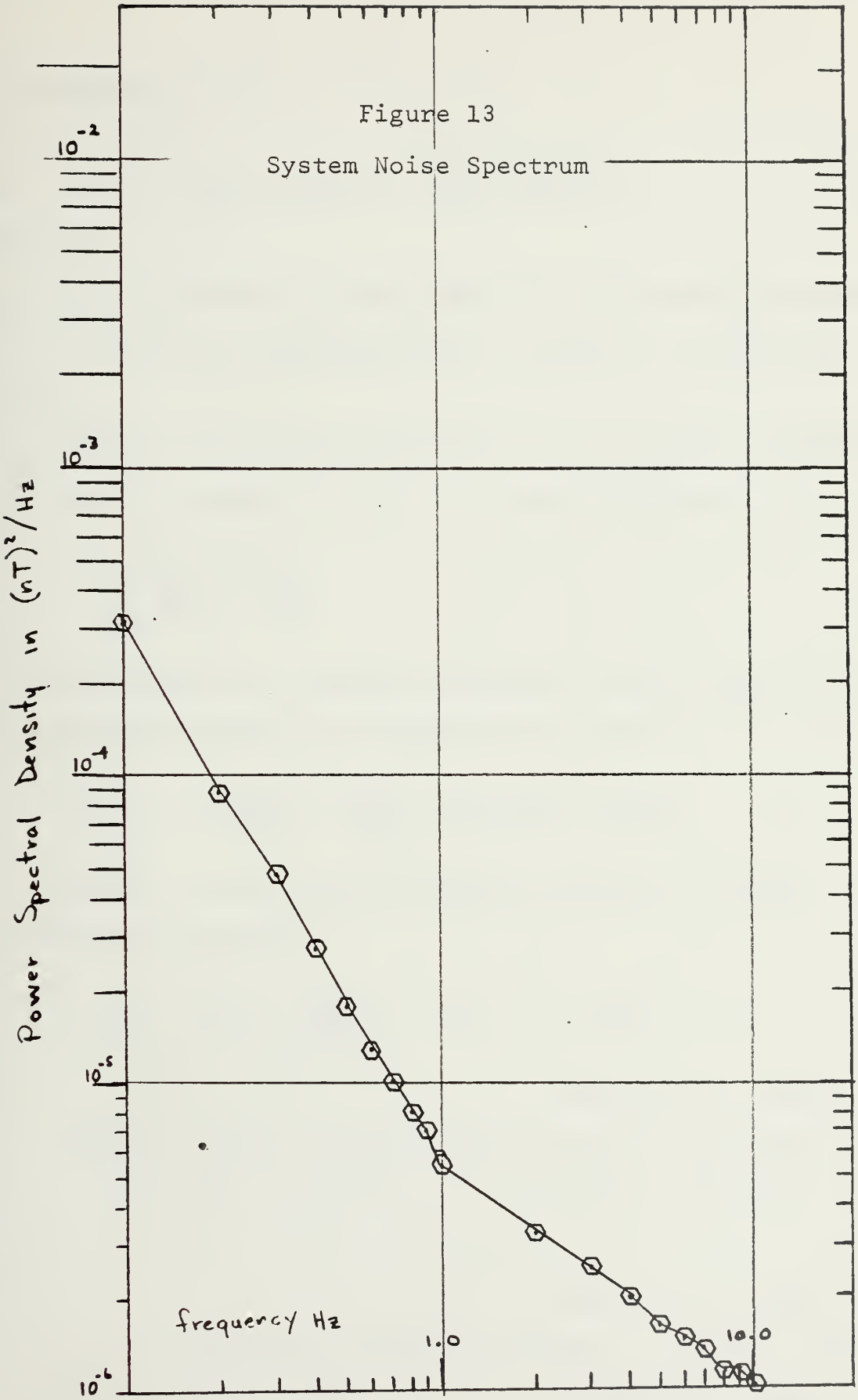

Calibration

Frequency Range .1 to 25.6 Hz

Window Function (Rectangular) 0dB correction

Input Signal

(a) The calibration of the signal out of the discriminator and the differential amplifier was 4 mV per Hz of frequency excursion.

(b) Filter gain was accomplished by an amplifier within the filter and was a factor of 10.5 X. Thus the signal was

$$10.5\left(\frac{4mV}{Hz}\right) = \frac{42mV}{Hz}$$

(c) The cesium cell Larmor Frequency constant per nT of field intensity change is 3.499 Hz per nT, thus

$$\frac{42mV}{Hz} \cdot \frac{3.499Hz}{nT} = \frac{147mV}{nT} \quad \text{reference signal}$$

STEP 1: Relate input reference signal to 100 mV, the 0dB attenuation setting

$$147mV = 1nT \rightarrow \frac{100mV}{147mV} = .68:1 = -3.35dB: \quad 1nT$$

Correction -3.35dB

STEP 2: Read 3 correction factors from 1510 front panel

a. Frequency range .1 to 25.6 Hz - per Hertz correction

Correction +10dB

b. Required attenuator setting to prevent overload

Correction 0dB

c. Window function rectangular

ENBW = 1 Correction 0dB

STEP 3: Add all corrections in steps 1 to 3 for total correction

-3.35 dB
+10.00 dB
+6.65 dB TOTAL CORRECTION

This means that a signal corresponding to a 1nT change in field strength at the 1510 input will require correction of 6.65dB at 1510 output. Thus, on the C.R.O. $\frac{1(nT)^2}{Hz}$ is defined to be at the -6.65dB calibration mark. By relating the input signal to the 0dB level it is possible to calculate where 1nT lies on the y axis of the dB calibrated C.R.O. The corrections are necessary to take into account what scales, window and frequency range are being used.

IV. EXPERIMENTAL RESULTS

A. INTRODUCTION

In a series of preliminary tests and calibration runs, as outlined in the previous section, the suitability of the magnetometer and recording equipment to analyze geomagnetic fluctuations had been established. During the month of April, 1978, a total of 53 hours of data was recorded, covering various times of day and a range of geomagnetic activity from very quiet to moderately disturbed. Each data run was 85 minutes long from which 512 individual spectra were computed and then averaged. The width of each frequency "bin" was 0.1 Hz or 256 bins between .1 and 25.6 Hz. The averaged estimate of the spectrum of a random input signal has a Chi-squared distribution, having two times the selected number of averaged spectra degrees of freedom. The statistical characteristics result in a 95 per cent confidence that the estimate will be within a $\pm$.4dB accuracy for a 512 spectra average.

The observations made of the magnetic field in Monterey were most concerned with the 0.1 to 10.0 Hz frequency range. Each of the spectra taken the spectral power density for this range was computed and displayed. Comparisons were made of the spectral power density at one specific time frame for a number of days. Comparisons were also made of spectra taken at different times of the day, and of the spectral power densities as affected by varying degress of field activity.

B. TYPICAL SPECTRA

Figures 14 through 18 each represent the average of 512 spectra taken from a recording of the earth's magnetic field at various time periods during the day. Each curve is a typical spectrum for daily field variations during the time frames indicated.

Figures 19 through 21 illustrate the spectra of five 85 minute runs for local night (0000-0200), local morning (0800-1000) and local afternoon (1600-1800), showing the day to day variations in the spectra. All times are given as Pacific Standard Time.

Figures 22 through 24 are the averages of the five curves given in Figures 19, 20 and 21, except for local night, where only three of the five spectra were used. It was found that because one of the curves had significantly more power than the other four, and another of the curves had significantly less power, that it was decided not to include these two when computing the mean. Otherwise the high power spectrum would effectively be reproduced as the average spectrum.

Figure 25 illustrates the power spectra of the 1730 to 1930 period for an average day and for a magnetically disturbed day. The disturbed field has 10dB greater power level in the .1 to .6 Hz range. The spectra nearly duplicate each other from 3 Hz to 10 Hz. The Fredricksburg a index had a value of 7 at the disturbed recording time and a value of 3 at the time the lower power curve was taken. These index readings were

Figure 14

0000 - 0200 PST 11 April 1978

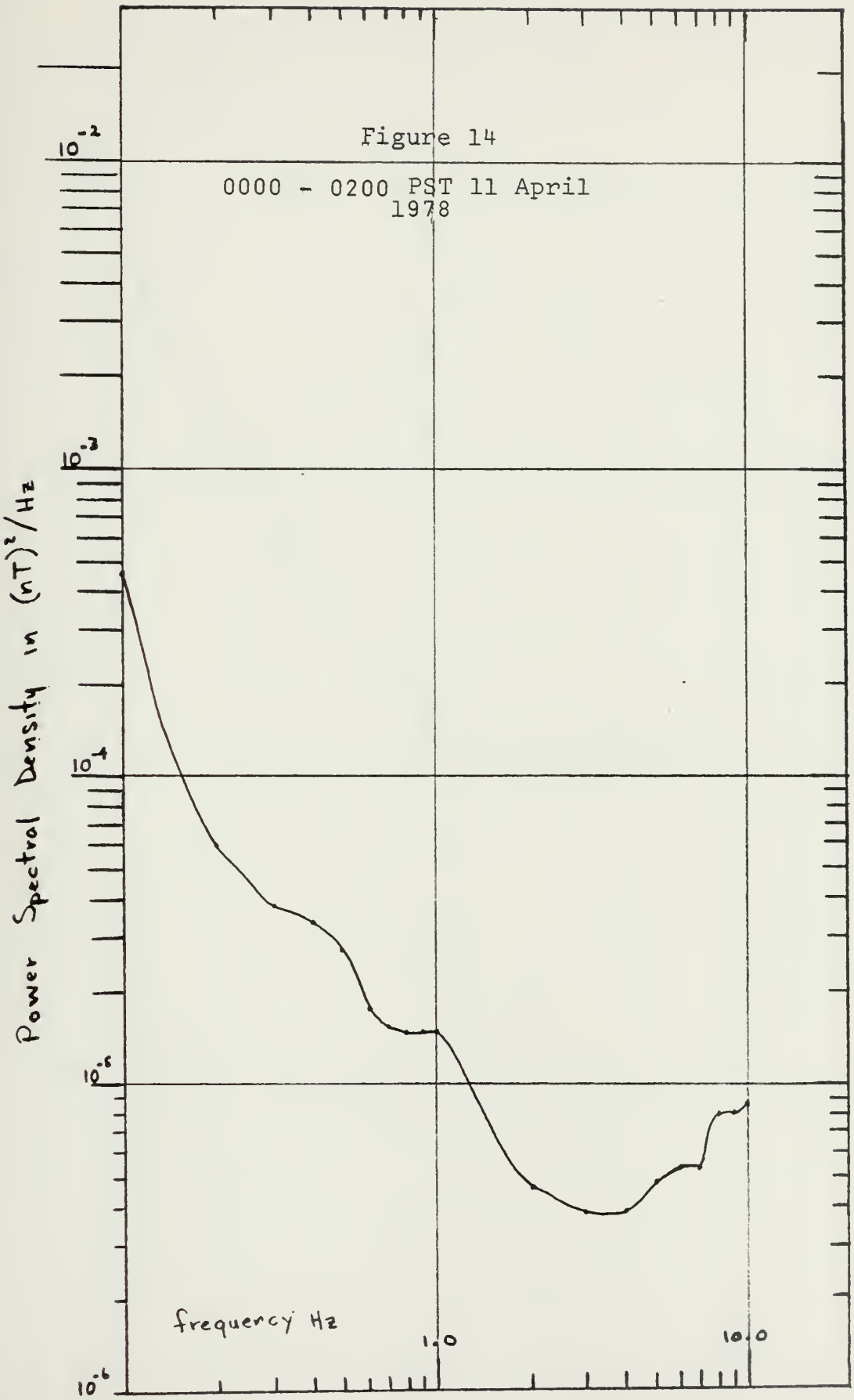

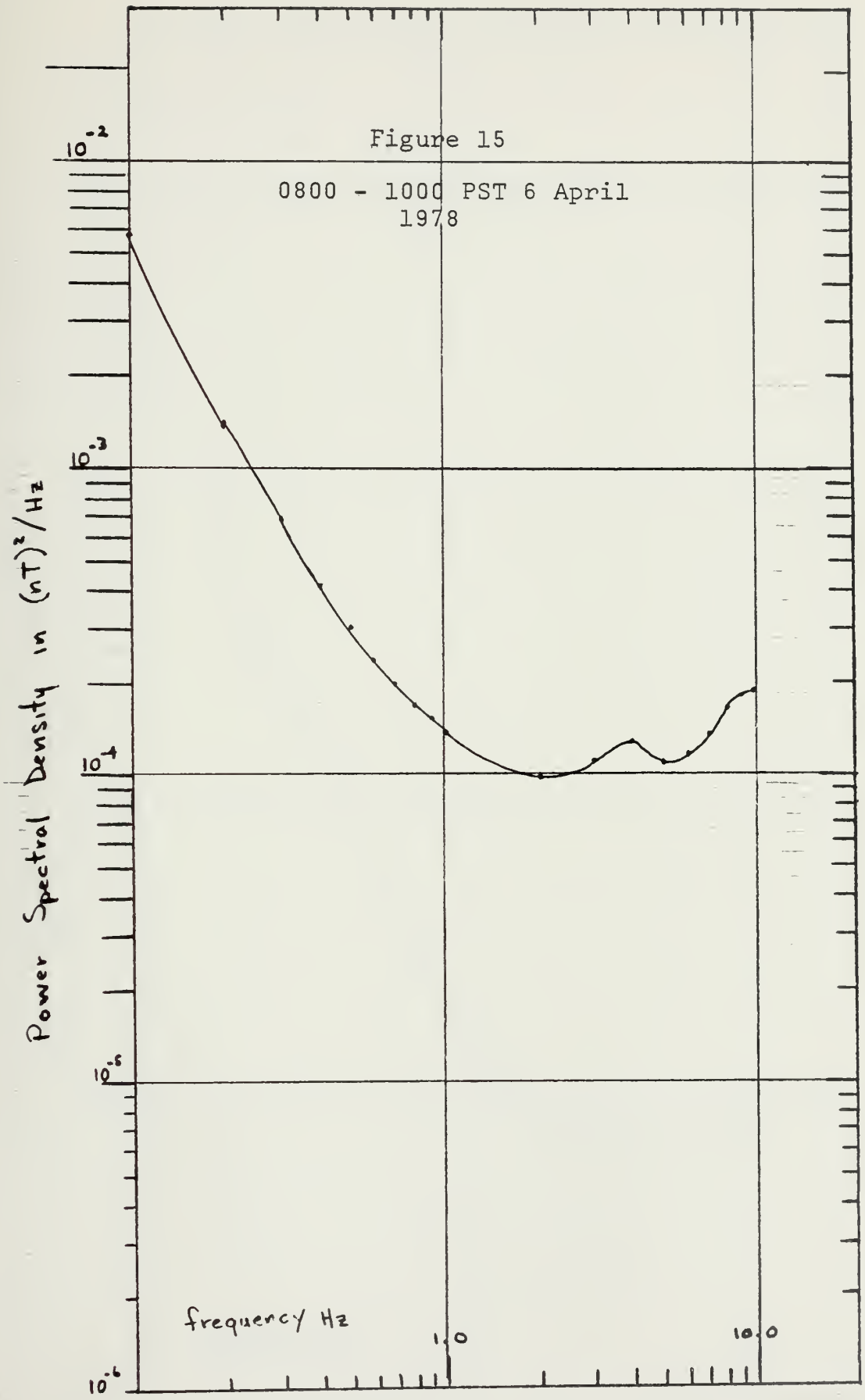
Figure 15
0800 - 1000 PST 6 April 1978
Power Spectral Density in $(nT)^2/Hz$
10^{-2}
10^{-3}
10^{-4}
10^{-5}
10^{-6}
frequency Hz
1.0
10.0

Figure 16

1300 - 1500 PST 13 April 1978

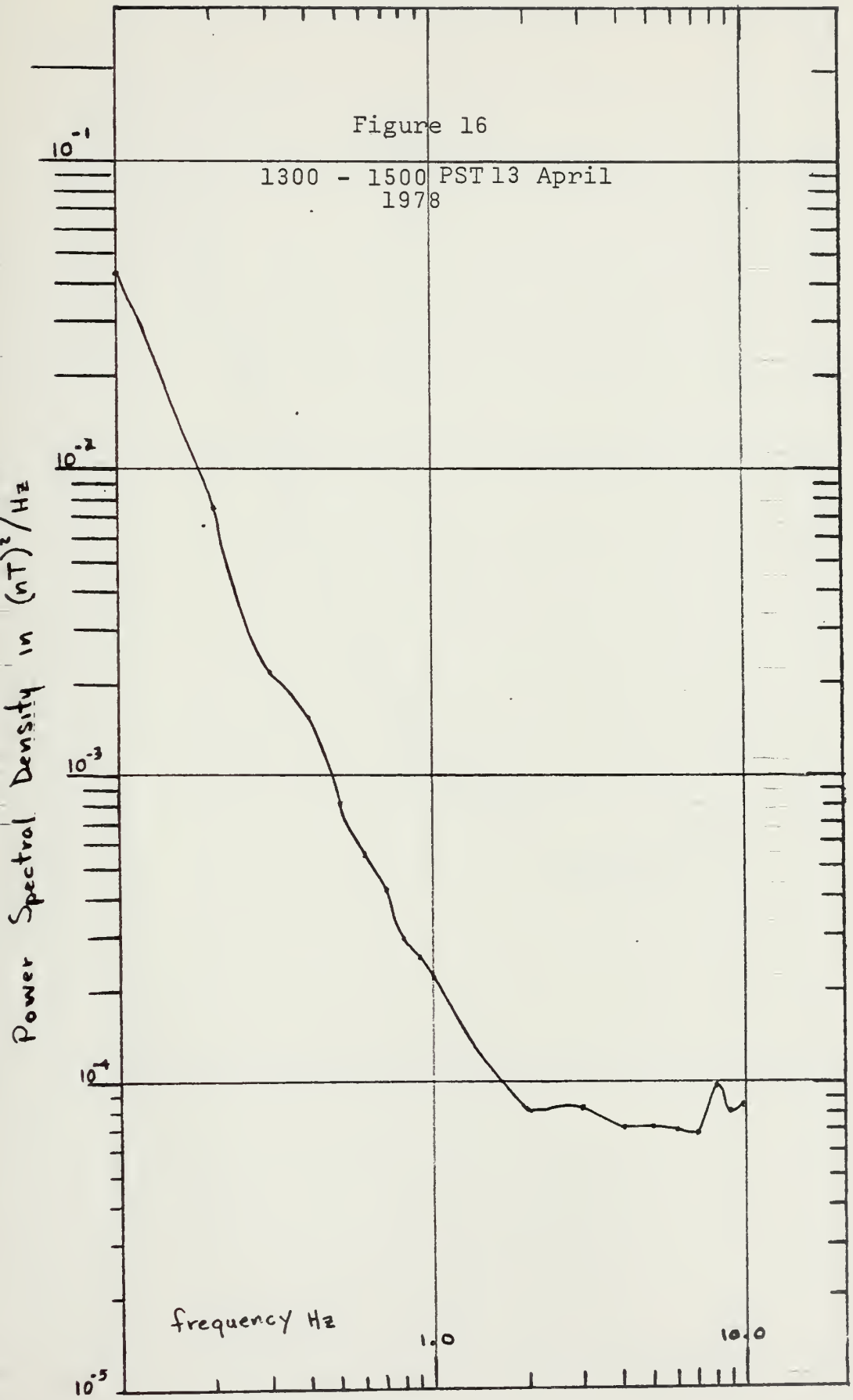

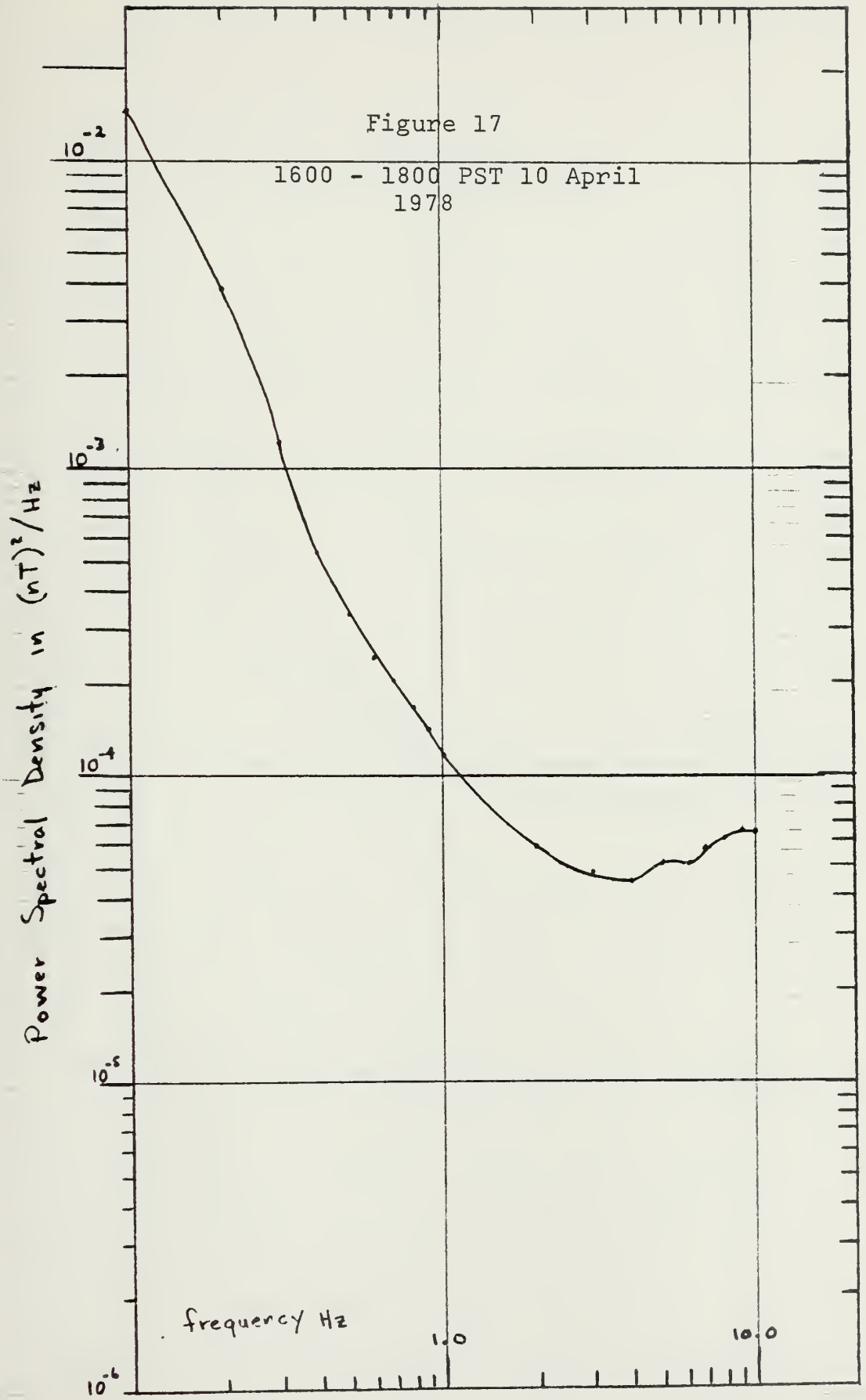
Figure 17
1600 - 1800 PST 10 April
1978
Power Spectral Density in $(nT)^2/Hz$
10^{-2}
10^{-3}
10^{-4}
10^{-5}
10^{-6}
frequency Hz
1.0
10.0

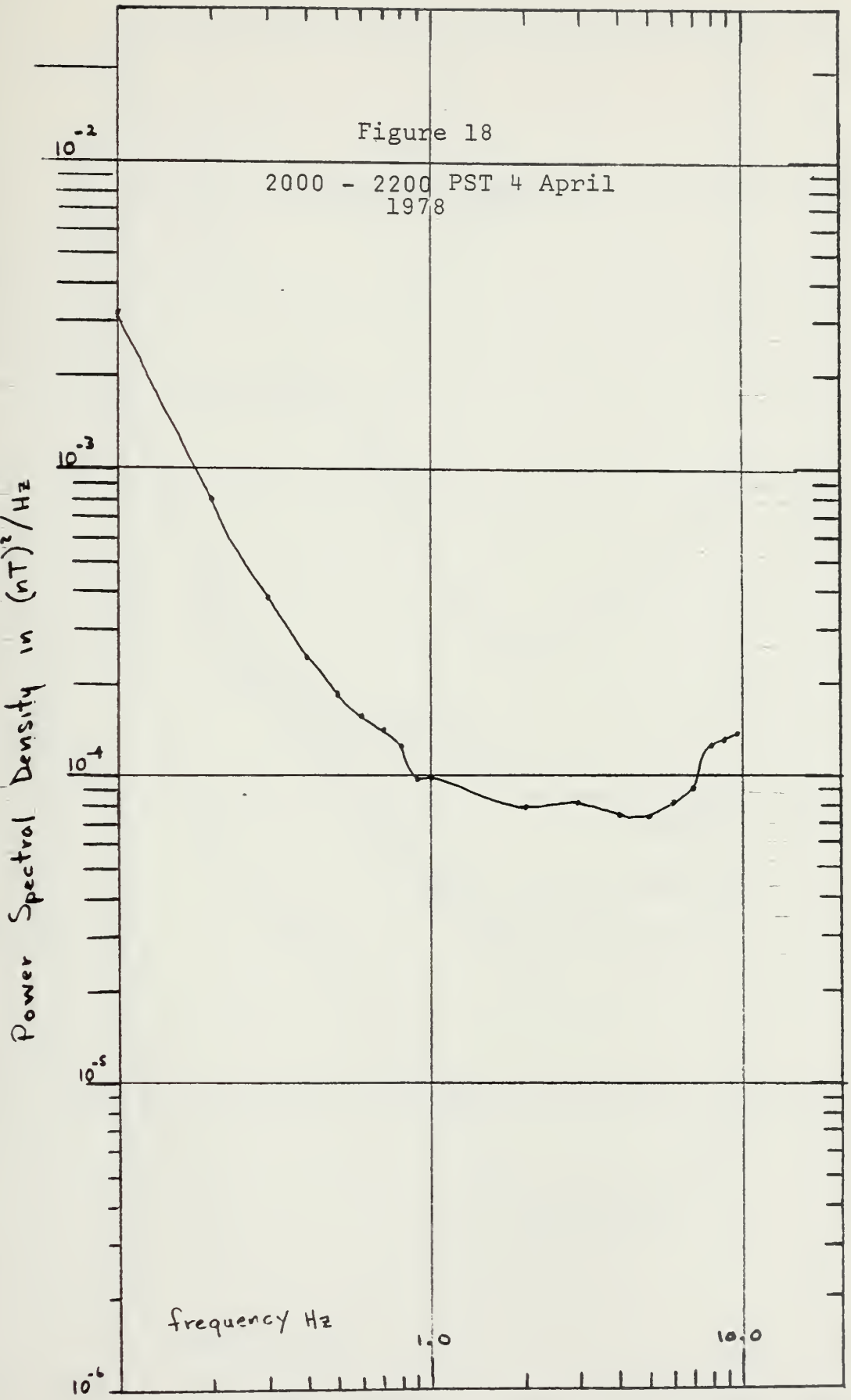
Figure 18
2000 - 2200 PST 4 April 1978
Power Spectral Density in $(nT)^2/Hz$
10^{-2}
10^{-3}
10^{-4}
10^{-5}
10^{-6}
frequency Hz
1.0
10.0

Figure 19

Local Night Spectra
(0000-0200)

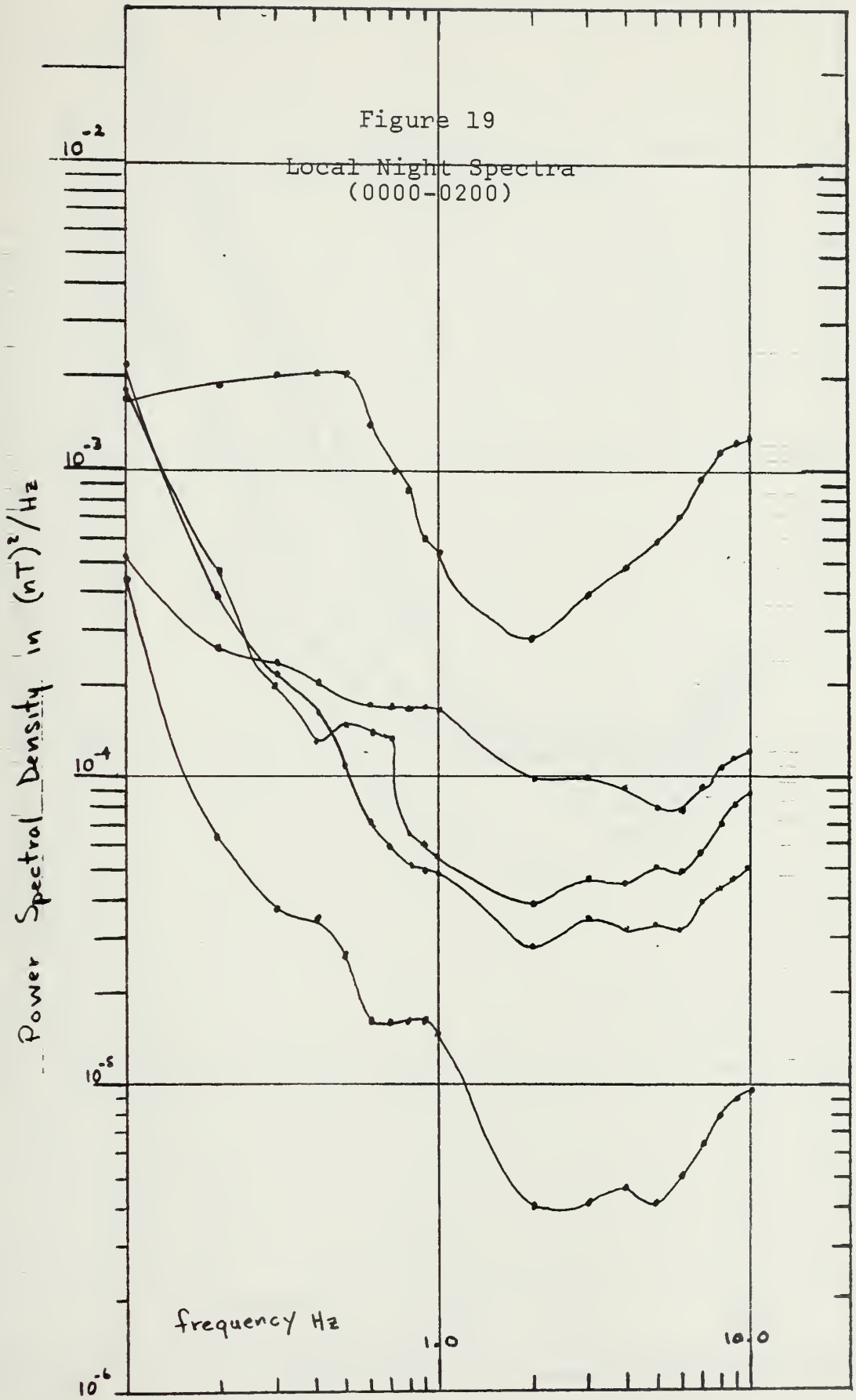

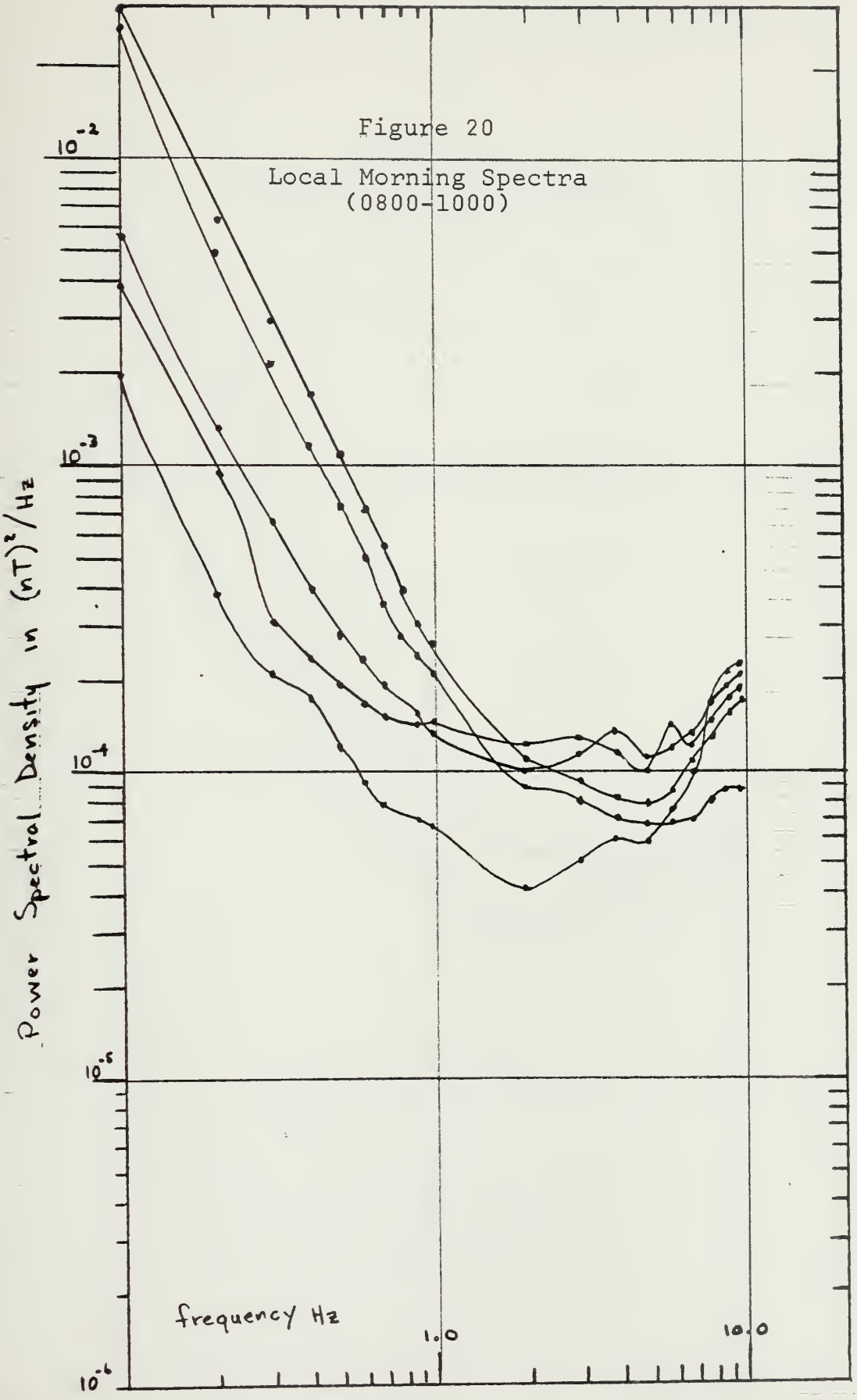
Figure 20
Local Morning Spectra
(0800-1000)
Power Spectral Density in $(nT)^2/Hz$
10^{-2}
10^{-3}
10^{-4}
10^{-5}
10^{-6}
frequency Hz
1.0
10.0

Figure 21

Local Afternoon Spectrum
(1600-1800)

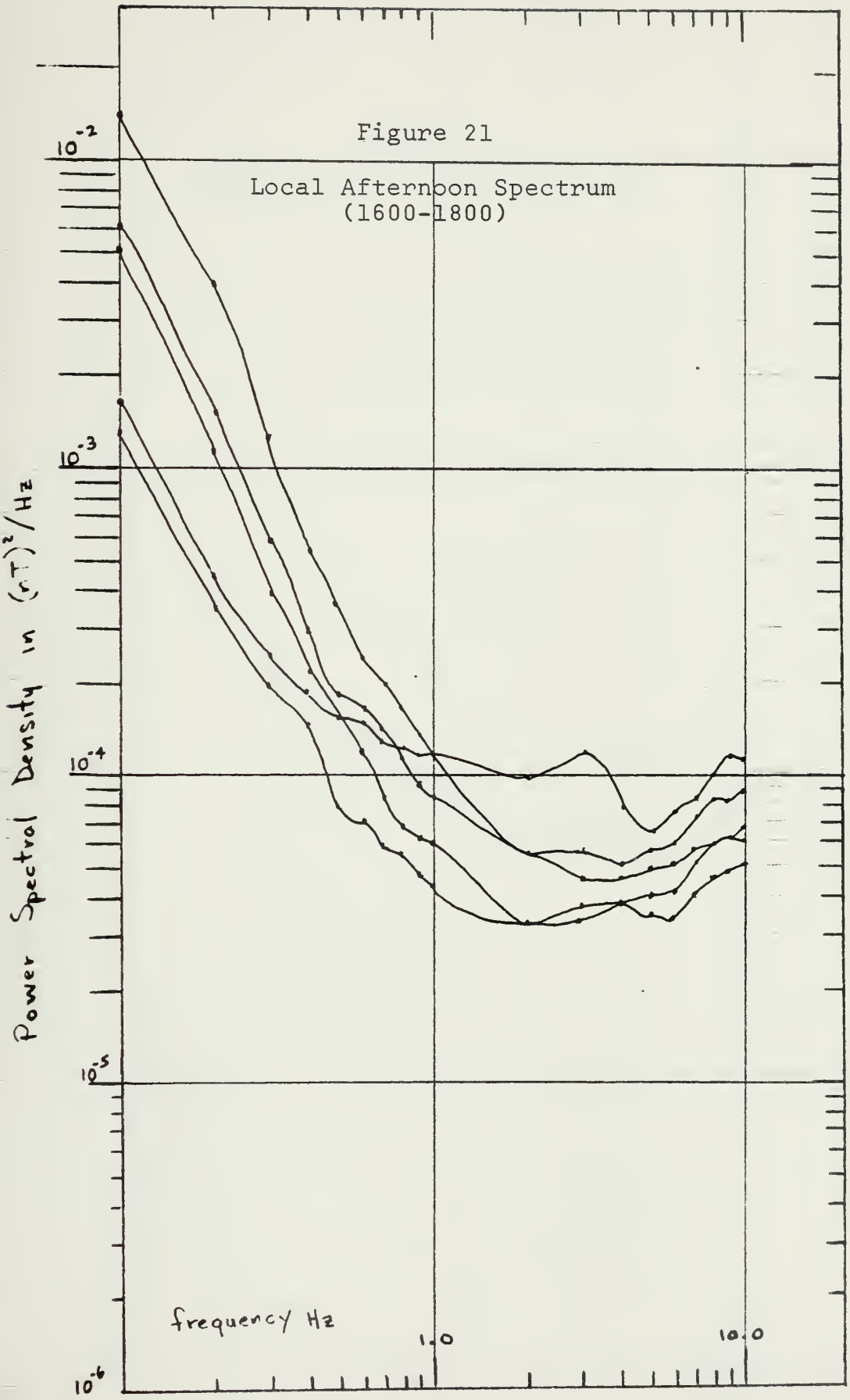

Figure 22

Average Local Night Spectrum

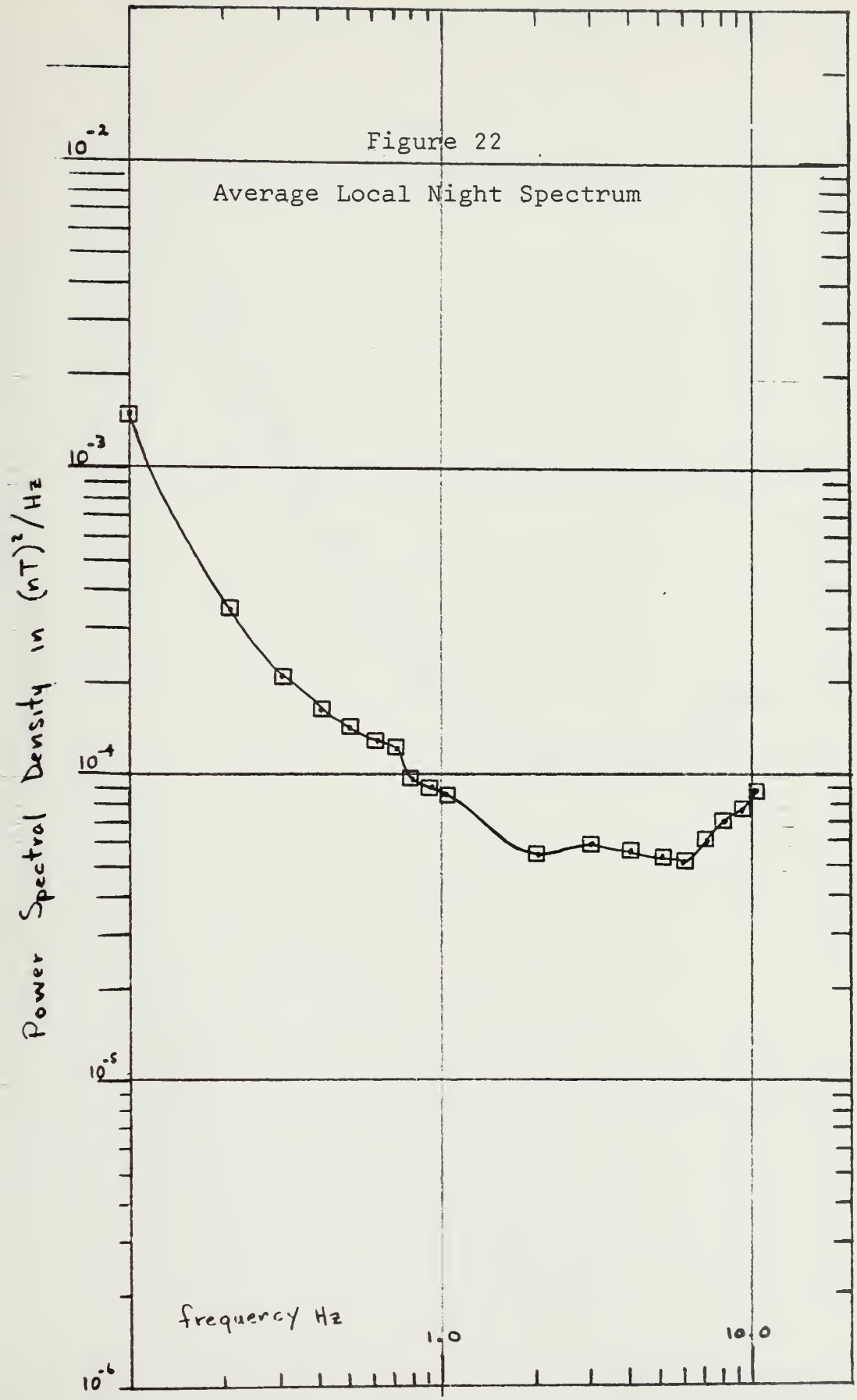

Figure 23

Average Local Morning Spectrum

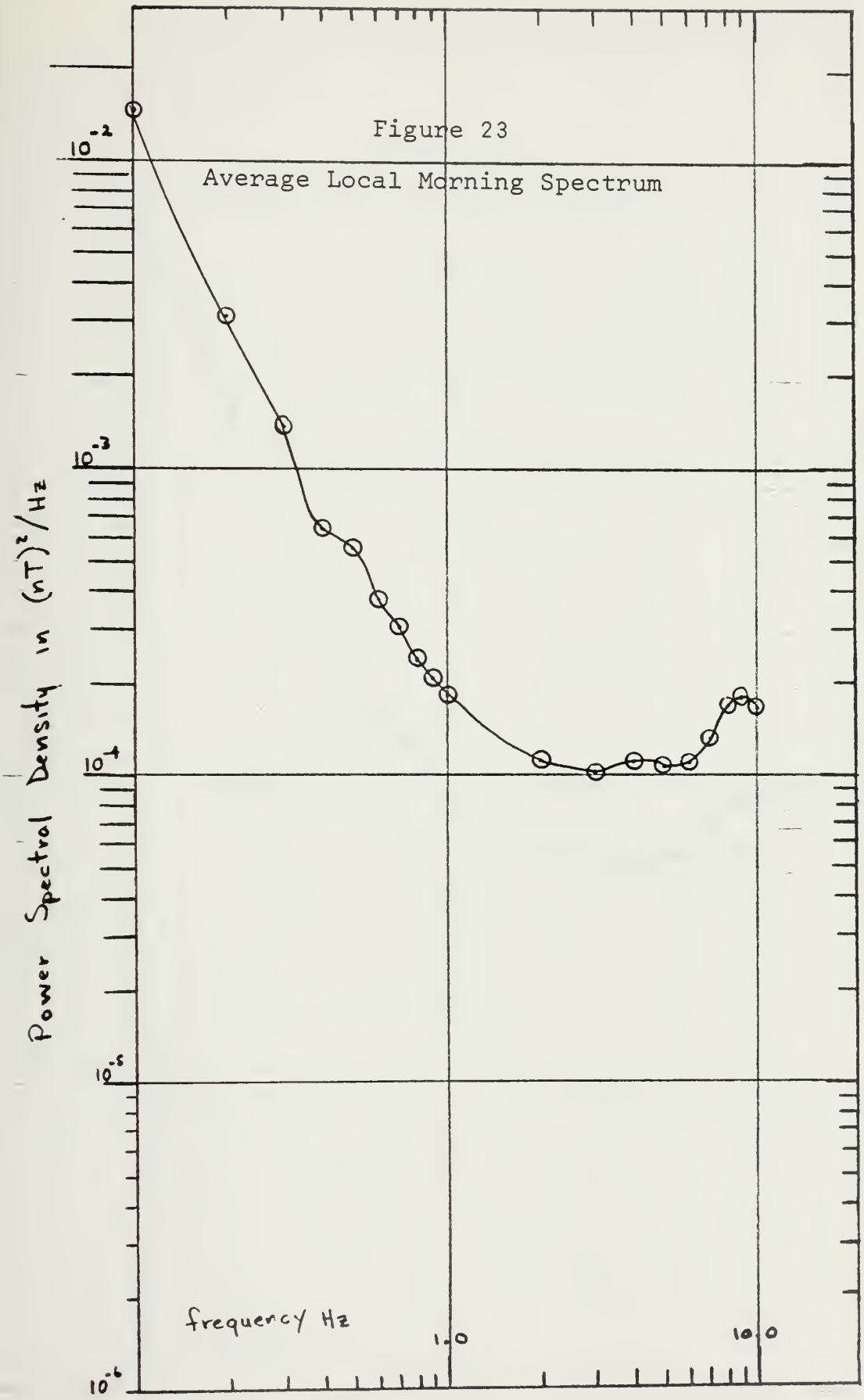

Figure 24

Average Local Afternoon Spectrum

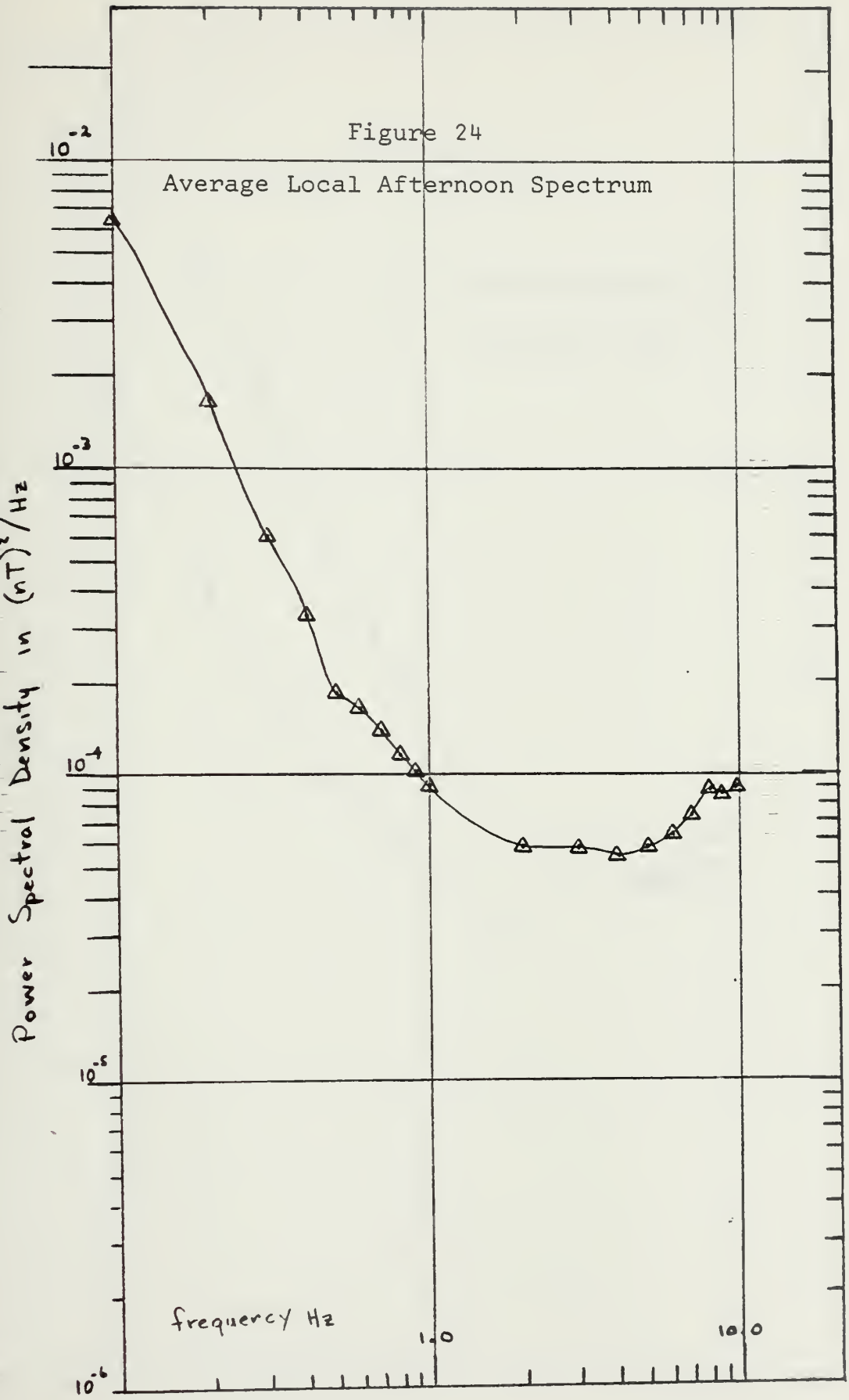

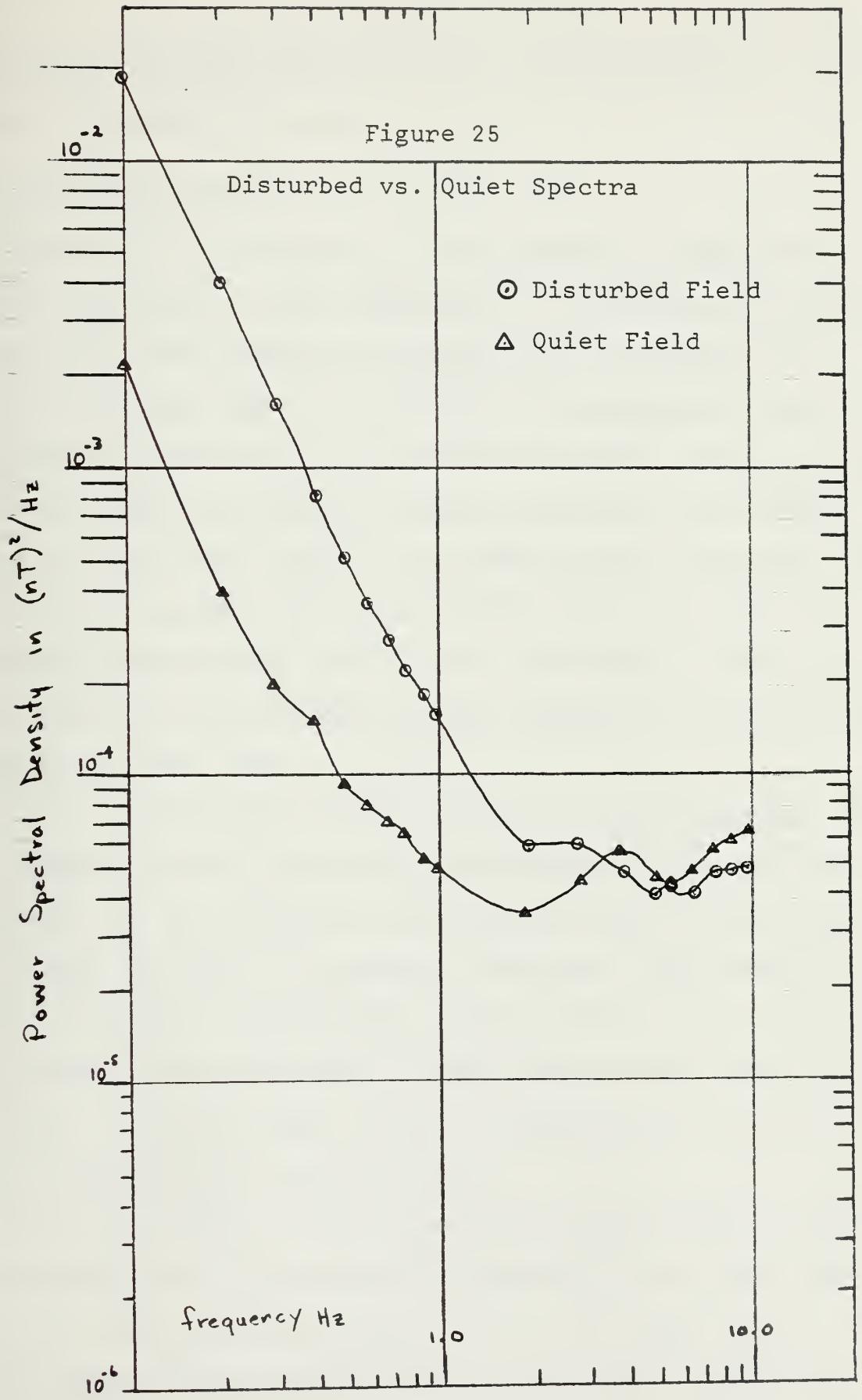
Figure 25
Disturbed vs. Quiet Spectra
Disturbed Field
Quiet Field
Power Spectral Density in $(nT)^2/Hz$
10^{-2}
10^{-3}
10^{-4}
10^{-5}
10^{-6}
frequency Hz
1.0
10.0

provided by the National Geophysical and Solar-Terestial Data Center in Boulder, Colorado.

C. COMPOSITE SPECTRA

Figure 26 is a composite of the important curves taken during the course of this experiment. It includes a five-day average for local morning and afternoon, and a three-day average for local night. In addition, the equipment noise spectrum is displayed. It is evident from this composite that the local night (0000-0200) spectrum approached the system noise spectrum most nearly of the three periods observed. The local night spectrum had significantly less power than the other two periods only in the .1 to .4 Hz range. From .5 Hz to 10.0 Hz all three average spectra exceeded the system noise level by at least 10dB.

Local morning and afternoon had very similar spectra. At most frequencies the two spectra were separated by only 3dB in power. At all frequencies the morning spectrum had slightly more power than did the afternoon spectrum. Both spectra displayed a definite -20dB/decade slope in the 0.1 to 1.0 Hz range. Both curves also exhibited a drastic slope change from 1.0 Hz to 10 Hz. Here the slope changed to positive at 4 Hz and then back to negative at the 10 Hz point.

The local night averaged curve had very low power at the low frequency end of the spectrum compared to the other two periods. This was true for the .1 to .4 Hz range. From .5 Hz to 10.0 Hz, the local night spectrum displayed the general

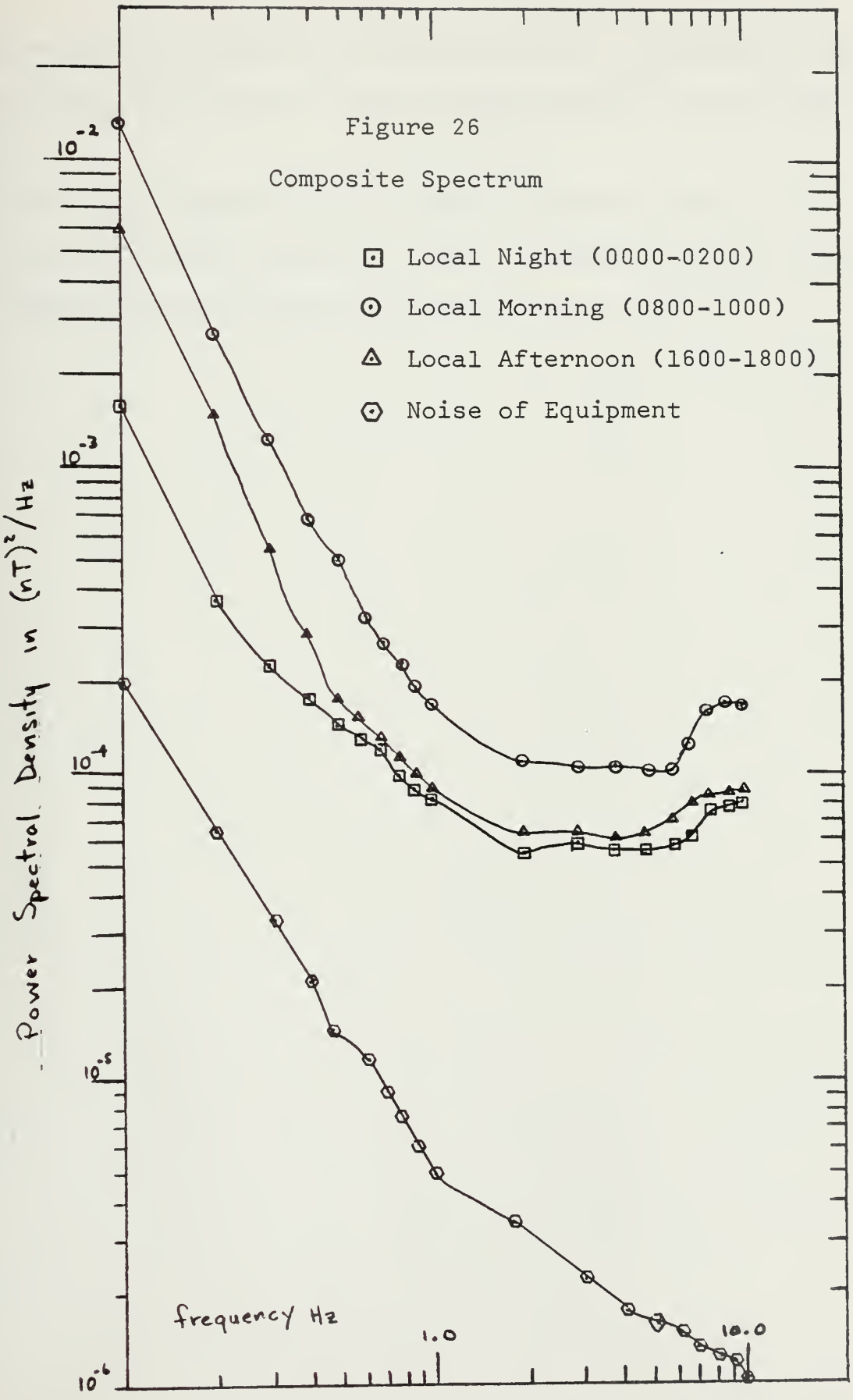
Figure 26
Composite Spectrum
Local Night (0000-0200)
Local Morning (0800-1000)
Local Afternoon (1600-1800)
Noise of Equipment
Power Spectral Density in $(nT)^2/Hz$
10^{-2}
10^{-3}
10^{-4}
10^{-5}
10^{-6}
frequency Hz
1.0
10.0

trend exhibited by the local morning curve. In general, the local night curve had the lowest power density for all frequencies.

The lowest signal to noise ratio occurred at the .3 Hz point where it had a value of 7.5dB. A signal to noise ratio of +10dB existed for all frequencies above .5 Hz.

V. CONCLUSIONS

A. DATA SUMMARY AND RECOMMENDATIONS

The characteristics of the spectra agree in general shape with those illustrated in the Trapped Radiation Handbook [Cladis, Davidson and Newkirk 1971], for the frequency range 0.1 to 10.0 Hz. The power levels at these frequencies agree in general with those observed earlier at Stanford [Fraser-Smith and Buxton 1975].

The average spectra illustrate the varying level of magnetic fluctuations as a function of time of day. For the time periods analyzed, it was observed that local night (0000-0200) had the lowest power density for each frequency measured. The local morning (0800-1000) spectrum exhibited the greatest power density for each frequency measured. The .1 Hz point of the local morning spectrum had the greatest power density ($4. \times 10^{-2}(nT)^2/Hz$). The 2 Hz point of the local night spectrum had the least power density recorded ($4. \times 10^{-6}(nT)^2/Hz$) thus spanning four orders of magnitude.

It was found that the three average spectra converged as frequency increased toward 10 Hz, where only 2dB in power separated the night time and morning power density levels.

During data collection, there were periods when the geomagnetic activity level was too low to record. At these times only the equipment noise spectrum was observable.

The data taken during the experiment and presented above is deemed reliable. However, in order to extract meaningful geophysical conclusions, it is necessary to collect and analyze a far greater amount of data for different times of the year, different times of the day and for varying degrees of geomagnetic activity levels. It is therefore recommended that these measurements be continued and expanded, preferably with the addition of digitizing equipment for computerized data handling and analysis.

B. EQUIPMENT IMPROVEMENTS RECOMMENDED

The Varian 4938 magnetometer system provided reliable magnetic field information in the 0.1 to 10.0 Hz frequency range. However, the frequency response of the system was not flat as initially anticipated, but rather rolled off by 8.5dB from 2.0 to 10.0 Hz. The cause of this roll off is suspected to lie in the mixer-discriminator circuitry since both sensors exhibit essentially the same performance properties.

The plotted power spectra did not show the same fine structure as observed on the C.R.O. This is primarily due to the plotter-analyzer interface. Some fine structure elements were lost in transmitting the analyzer C.R.O. display to the plotter, due to a response mismatch between the analyzer and plotter.

The single cell sensor was found to be reliable only when in a stable and stationary support. This type of sensor can not be allowed to have large angular motion, and must have stability in its orientation to the total field vector for optimum signal to noise characteristics.

The tape recording of the magnetometer data allowed for permanent record keeping of the data but contributed some noise to the system. The flutter compensation circuit cancelled out much of the vibration noise and a good reproduction of the magnetometer discriminator output was thus achieved to within $\pm$ 2dB. A digital data collection scheme could greatly improve the absolute accuracy of the field measurements and eliminate the discriminator circuitry and its associated noise.

LIST OF REFERENCES

1. Blackman, R.B. and Tukey, J.W., The Measurement of Power Spectra, Dover Publ., 1968.

2. Bloom, A.L., "Optical Pumping", Scientific American, Oct. 1960.

3. Bloom, A.L., "Principles of Operation of the Rubidium Vapor Magnetometer", Applied Optics, V. 1, No. 1, p. 61-68, January 1961.

4. Campbell, W.H. and Matsushita, S., Physics of Geomagnetic Phenomena, V. 1,2, Academic Press, 1967.

5. Cladis, J.B., Davidson, G.T. and Newkirk, L.L., The Trapped Radiation Handbook, DNA 2542 H, 1971.

6. Davidson, M.J., "Average Diurnal Characteristics of Geo magnetic Power Spectrums in Period Range 4.5 to 1000 Seconds", Journal of Geophysical Research, V. 69, No. 23, p. 5116-5119, December 1964.

7. Dehmelt, H.G., "Modulation of a Light Beam by Precessing Absorbing Atoms", Physical Review, V. 105, No. 6, p. 1924-1925, January 1975.

8. Fraser-Smith, A.C. and Buxton, J.L., "Superconducting Magnetometer Measurements of Geomagnetic Activity in the 0.1 to 14 Hz Frequency Range", Journal of Geophysical Research, V. 80, No. 27, p. 3141-3147, August 1975.

9. Herron, T.J., "An Average Geomagnetic Power Spectrum for Period Range 4.5 to 12,900 Seconds", Journal of Geophysical Research, V. 72, No. 2, p. 759-761, January 1967.

10. Jacobs, J.A., Geomagnetic Micropulsations, 179 p., Springer, New York, 1970.

11. Fraser-Smith, A.C. et al., "Air/Undersea Communications at ULF using Airborne Loop Antennas, Stanford Elec. Lab TR-4207-6, 1977.

12. Naval Surface Weapons Center, White Oak Laboratory TR 77-41, Electromagnetic Background Noise in the Ocean Due to Geomagnetic Activity in the Period Range .5 to 1000 Seconds, by M.B. Kraichman, March 1977.

13. Naval Underwater Systems Center, Newport, Rhode Island T.R. 5681, ELF Effective Noise Measurements Taken in Connecticut During 1976, by Peter R. Bannister, 1977.

14. Pacific Sierra, Research TR 706, Land to Seafloor Electromagnetic Transmissions in the 0.1 to 10.0 Hz Band, by E.C. Field et al., August 1977.

15. Santirocco, R.A. and Parker, D.G., "The Polarization and Power Spectrum of Pc Micropulsations in Bermuda", Journal of Geophysical Research, V. 68, p. 5543, 1963.

16. Schumann, W.O. and König, H., "Über die Beobachtung von 'Atmospherics' bei geringsten Frequenzen", Naturwissenschafften, V. 41, p. 183, 1954.

17. Wertz, R., and Campbell, W.H., "Integrated Power Spectra of Geomagnetic Field Variations with Periods of .3 to 300 Seconds", Journal of Geophysical Research, V. 81, No. 28, p. 5131-5135, 1976.

18. Xefteris, C.L., A Magnetometer Data Acquisition System, M.S. Thesis, Naval Postgraduate School, Monterey, California, 1976.

INITIAL DISTRIBUTION LIST

		No. Copies
1.	Defense Documentation Center Cameron Station Alexandria VA 22314	2
2.	Library, Code 0142 Naval Postgraduate School Monterey CA 93940	2
3.	Department Chairman, Code 61 Department of Physics and Chemistry Naval Postgraduate School Monterey CA 93940	2
4.	Professor O. Heinz, Code 61Hz Department of Physics and Chemistry Naval Postgraduate School Monterey CA 93940	2
5.	LT John M. Barry N.E.T.C. Newport Surface Warfare Officers School Command Newport RI 02840	1
6.	Professor Paul M. Moose, Code 61Me Department of Physics and Chemistry Naval Postgraduate School Monterey CA 93940	1
7.	Professor George Sackman, Code 62Sa Department of Electrical Engineering Naval Postgraduate School Monterey CA 93940	1
8.	Dr. Robert Andrews, Code 463 Office of Naval Research 800 N. Quincy Street Arlington VA 22202	1
9.	Professor R. Helliwell Department of Electrical Engineering Stanford University Stanford CA 94305	1

Thesis
B2421
c.1

176510

Barry

Power spectra of geo-
magnetic fluctuations
between 0.1 and 10.0 Hz.